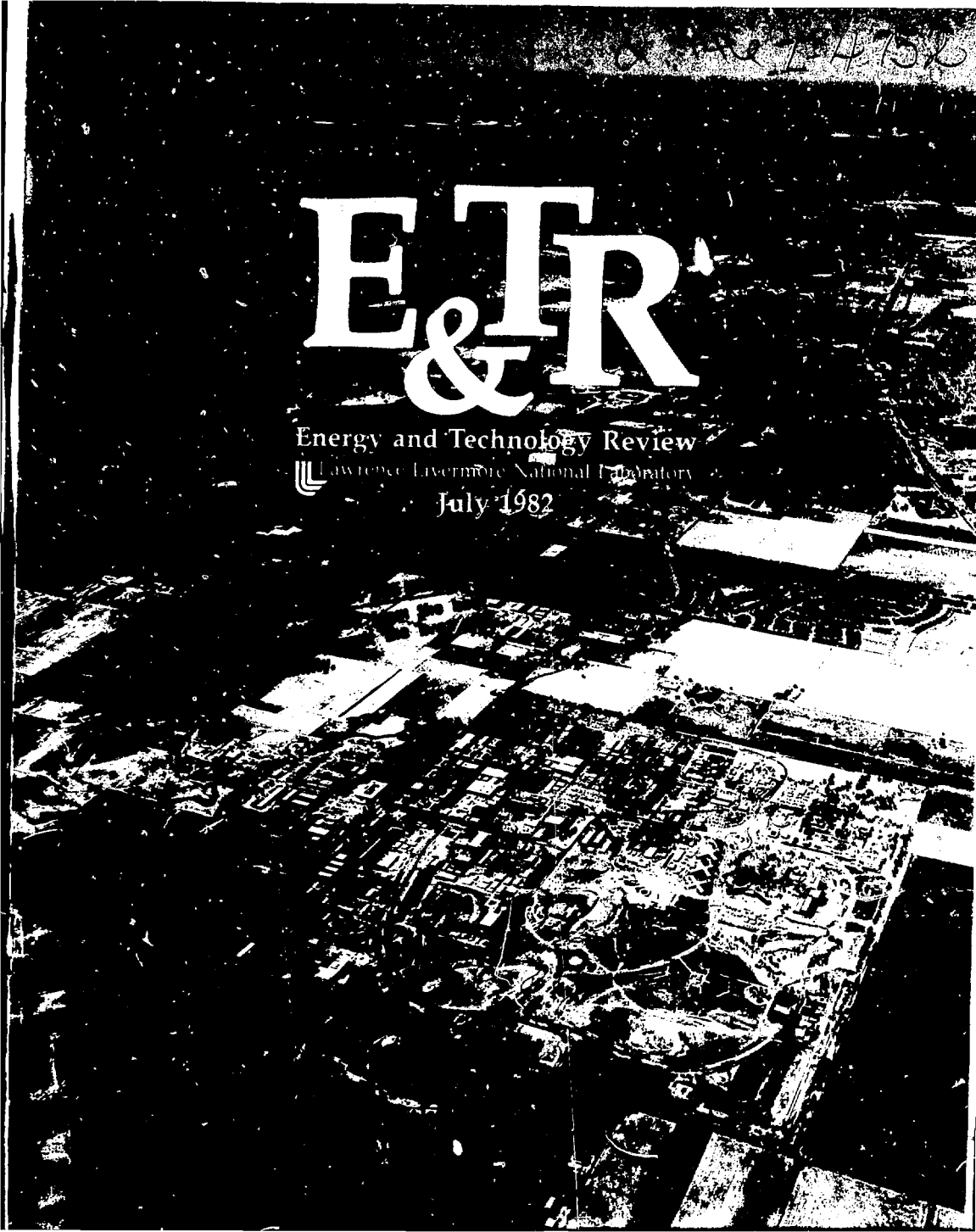
E&TR
Energy and Technology Review
Lawrence Livermore National Laboratory
July 1982

Prepared for **DOE** under contract
No. W-7405-Eng-48

About the Cover

Aerial view of the Laboratory looking west, the southern arm of the San Francisco Bay and the peninsula hills beyond can be seen at the top of the photograph. Each year LLNL Director Roger Batzel reports to the staff on the state of the Laboratory and the achievements of the past year. On June 9, 1982, Dr. Batzel reported on the estimated budget for the 1983 fiscal year and on recent trends in our major programs. The articles in this issue highlight Dr. Batzel's talk and describe some of the past year's accomplishments.

About the Journal

The Lawrence Livermore National Laboratory, operated by the University of California for the United States Department of Energy, was established in 1952 to conduct nuclear weapons and controlled thermonuclear reaction research. Today, about 60% of our resources are devoted to defense programs, which include weapons- and laser-fusion research. Other major areas of focus are magnetic fusion energy; laser isotope separation; chemistry, engineering, and physics research; biomedical and environmental sciences; applied energy technology; and work for other federal agencies. The *Energy and Technology Review* is published monthly to report on accomplishments in unclassified programs. A companion journal, the *Research Mondiale*, reports on weapons research and other classified programs. Titles from recent issues of the *Energy and Technology Review* are listed opposite the inside back cover.

Scientific Editor
Irving F. Stowers

General Editors
Richard B. Crawford
Mary Ann Esser
Patricia L. Lien
Eleanor O'Neal
Palmer Van Dyke

Graphics Designer
John Schuster

Production Staff
Louisa Cardoza
Dianne Carlson

UCRL--52000-82-7

DE82 019880

Energy and Technology Review

Lawrence Livermore National Laboratory

July 1982

UCRL-52000-82-7
Distribution Category UC-2
July 1982

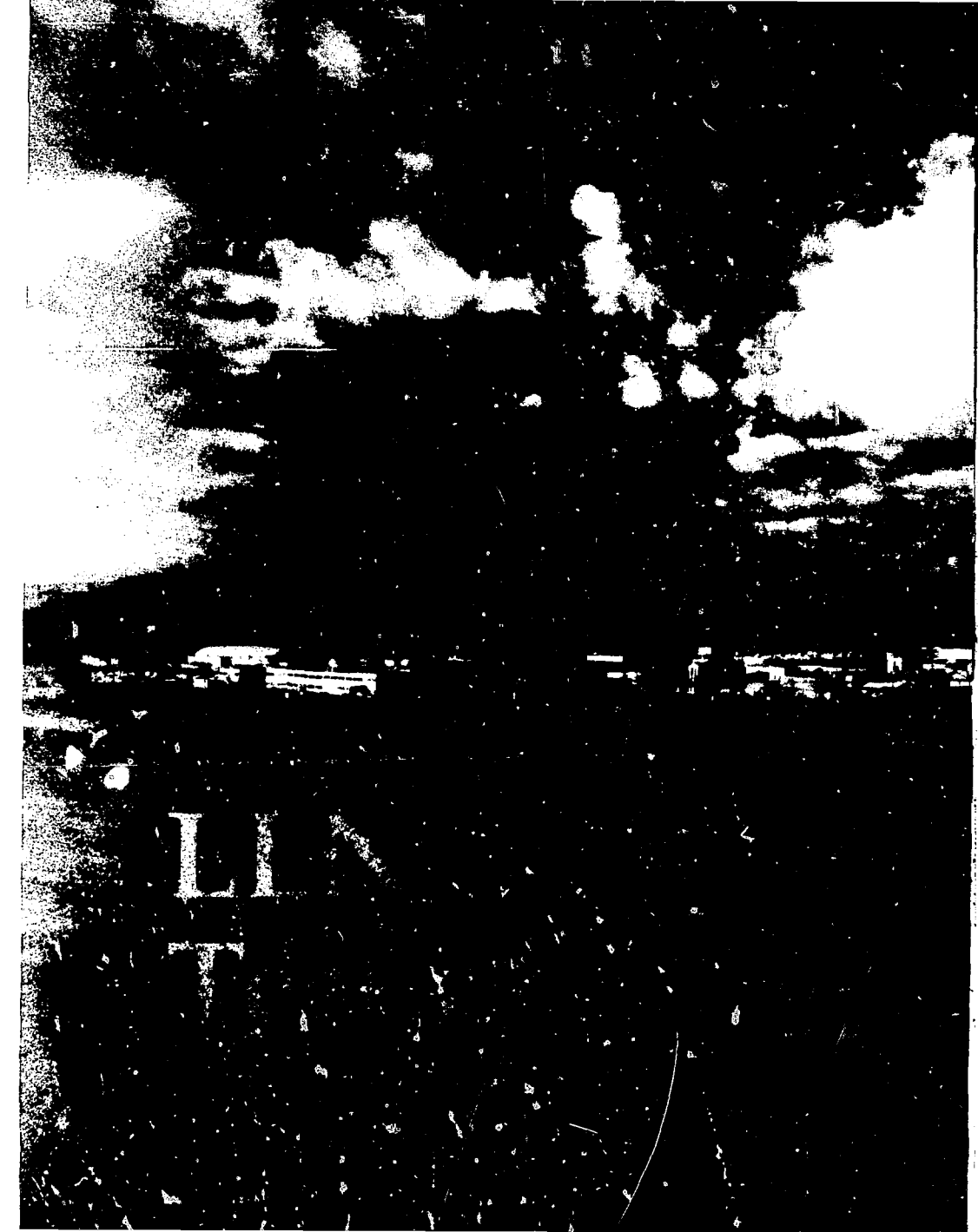
LI
T

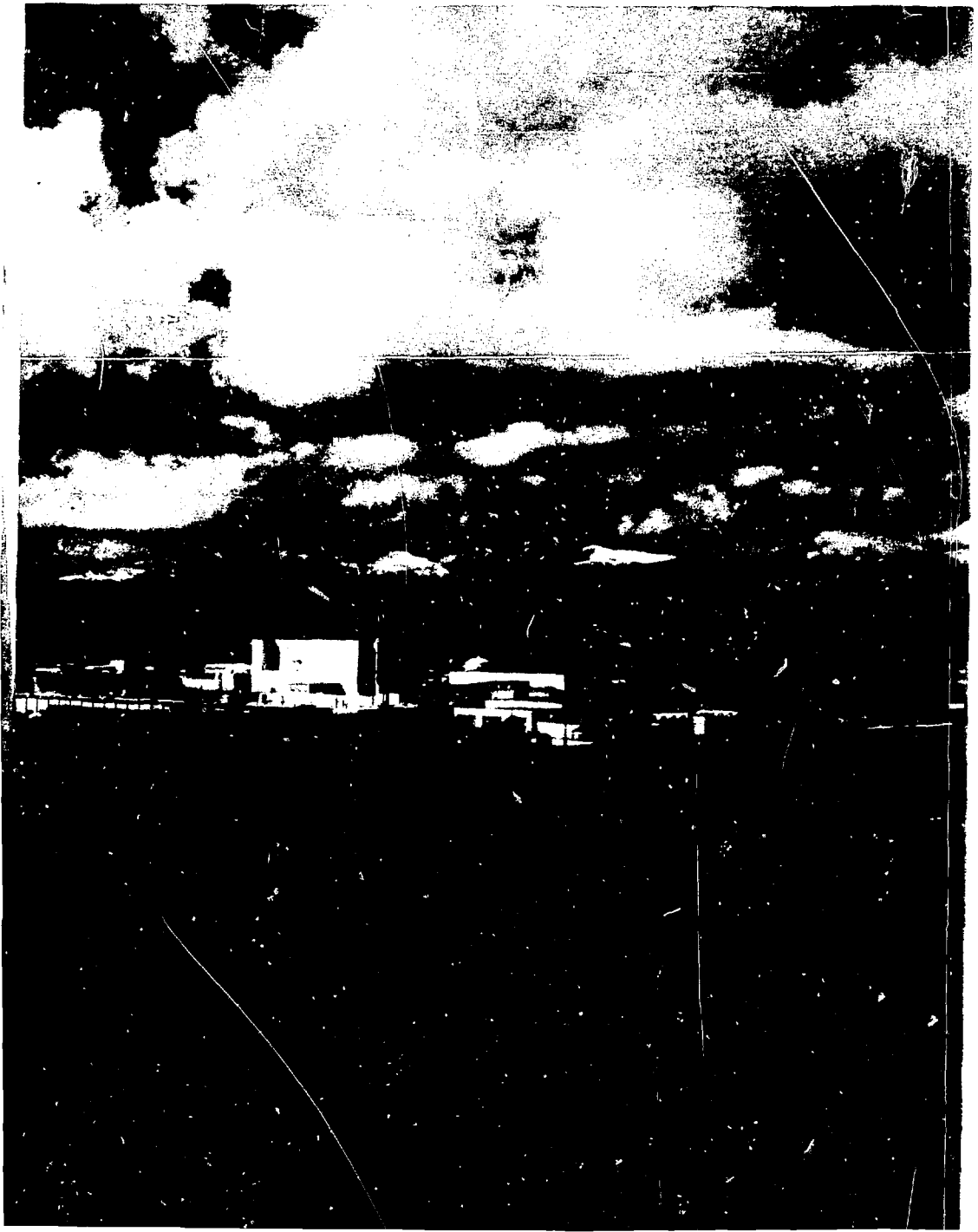

To the task of weapons development, the Laboratory applies a wide spectrum of resources and skills drawn from scientific, engineering, and technical disciplines.

The energy produced in thermonuclear weapons derives, in large part, from the energy of thermonuclear fusion. We can produce and study fusion reactions in a controlled environment by bringing a tiny deuterium-tritium fuel pellet to very high temperatures and densities in such a short time that the thermonuclear fuel will ignite and burn before the compressed core disassembles. This technique, known as inertial confinement, relies upon a driver (e.g., a laser) to deliver the extremely high-power, short-duration burst of energy required. Our inertial-confinement fusion program has both civil goals, for producing electricity, and military goals, for obtaining data on nuclear weapons physics and creating a source of radiation to simulate the effects of nuclear weapons on military hardware without conducting an actual nuclear test.

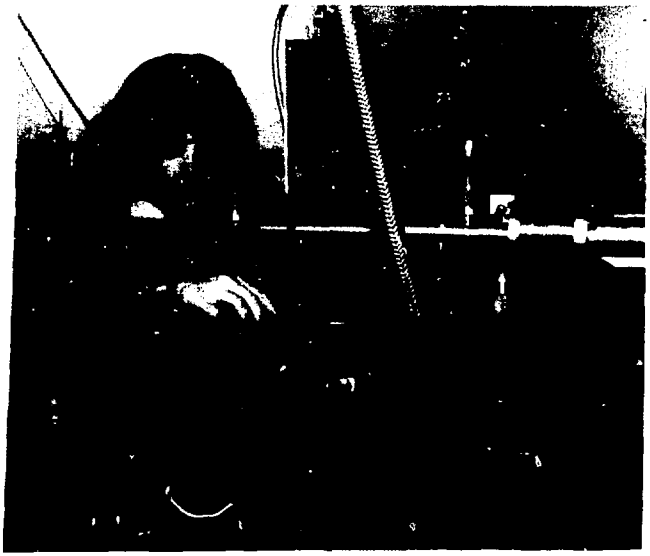

There are other ways of controlling fusion reactions. One approach is to rely upon specially shaped magnetic fields to confine the thermonuclear fuel while heating it to fusion temperatures and densities by some external means. LLNL is conducting a vigorous magnetic fusion research program, with the goal of developing the technology needed to harness thermonuclear fusion for power production. Successful development of a fusion reactor would give us practical access to fuels—deuterium (from water) and lithium—that will last for millennia. This program, which achieved several important goals during the past year, reflects our continued efforts to help meet future energy needs while maintaining the quality of the biosphere.

We are also exploring the use of lasers for separating one particular isotope of an element from other isotopes of that same element; this year, the atomic vapor laser isotope separation process, which we have been developing for the separation of uranium

isotopes, was selected by the Department of Energy for large-scale development. Other energy-related programs focus on such applied energy technologies as coal gasification and high-performance electric batteries that could power motor vehicles.

Our biomedical and environmental sciences programs explore sources of energy-related pollutants (both nuclear and nonnuclear), their methods of transport, and their effects on plants, animals, and humans. Studies range from investigations of the mechanisms of cellular change to extensive surveys of entire ecosystems and the safe, long-term storage of radioactive wastes.

The major research programs at LLNL can call upon a pool of specialized professionals and a constantly evolving supply of supporting technologies that are provided by a variety of internal support groups. These departments are defined for the most part in terms of areas of technical specialization (chemistry, physics, engineering, computations, etc.) and keep pace with developments in the various disciplines. The sophisticated theoretical and experimental projects these support departments carry out have applications that serve not only the major LLNL programs but also the interests of the broader technical community.

The timely availability of programmatic resources in personnel and material is supported by various administrative departments that are coordinated through five managers under the aegis of an associate director responsible for administration.

This issue of the *Energy and Technology Review* explores the technical horizons being defined by LLNL researchers in support and programmatic roles. Featured first is a summary of the annual State of the Laboratory address presented by the Director, Dr. Roger Batzel, on budgetary trends and the prospects for the future. Next is a sampling of Laboratory achievements, grouped under the three headings of national defense, energy and the environment, and supporting technologies.

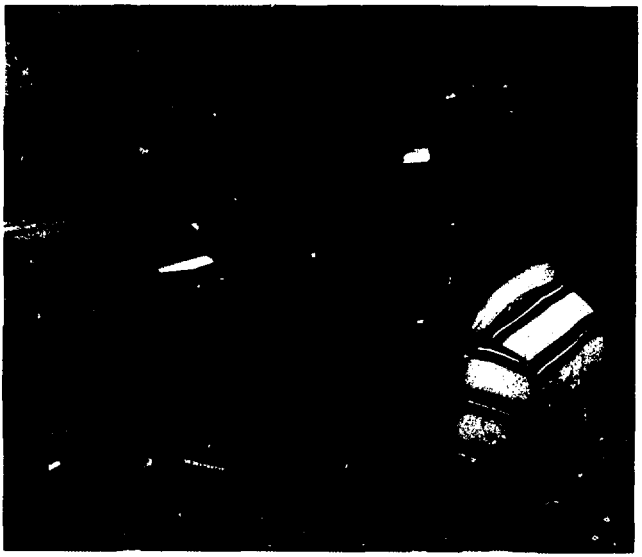

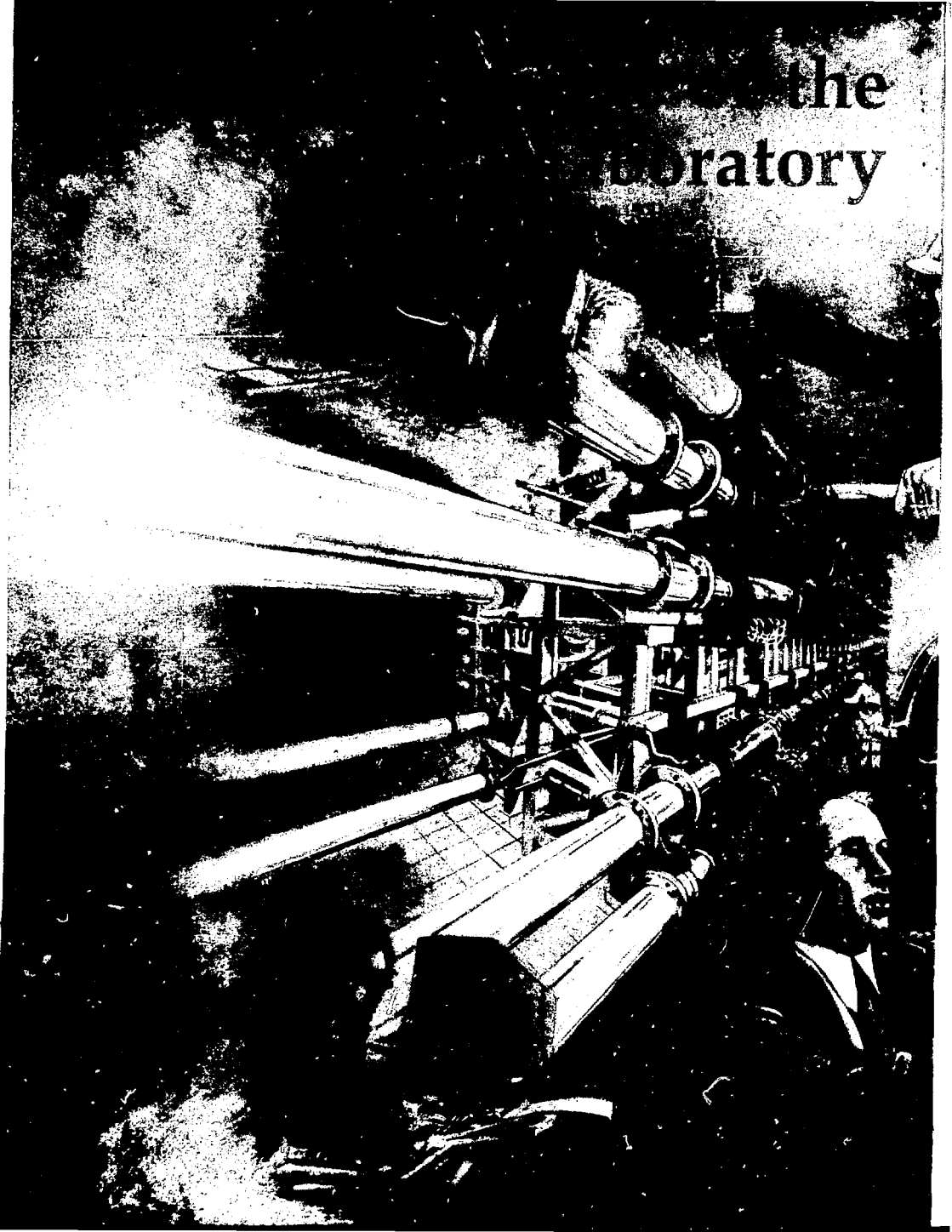
the
oratory

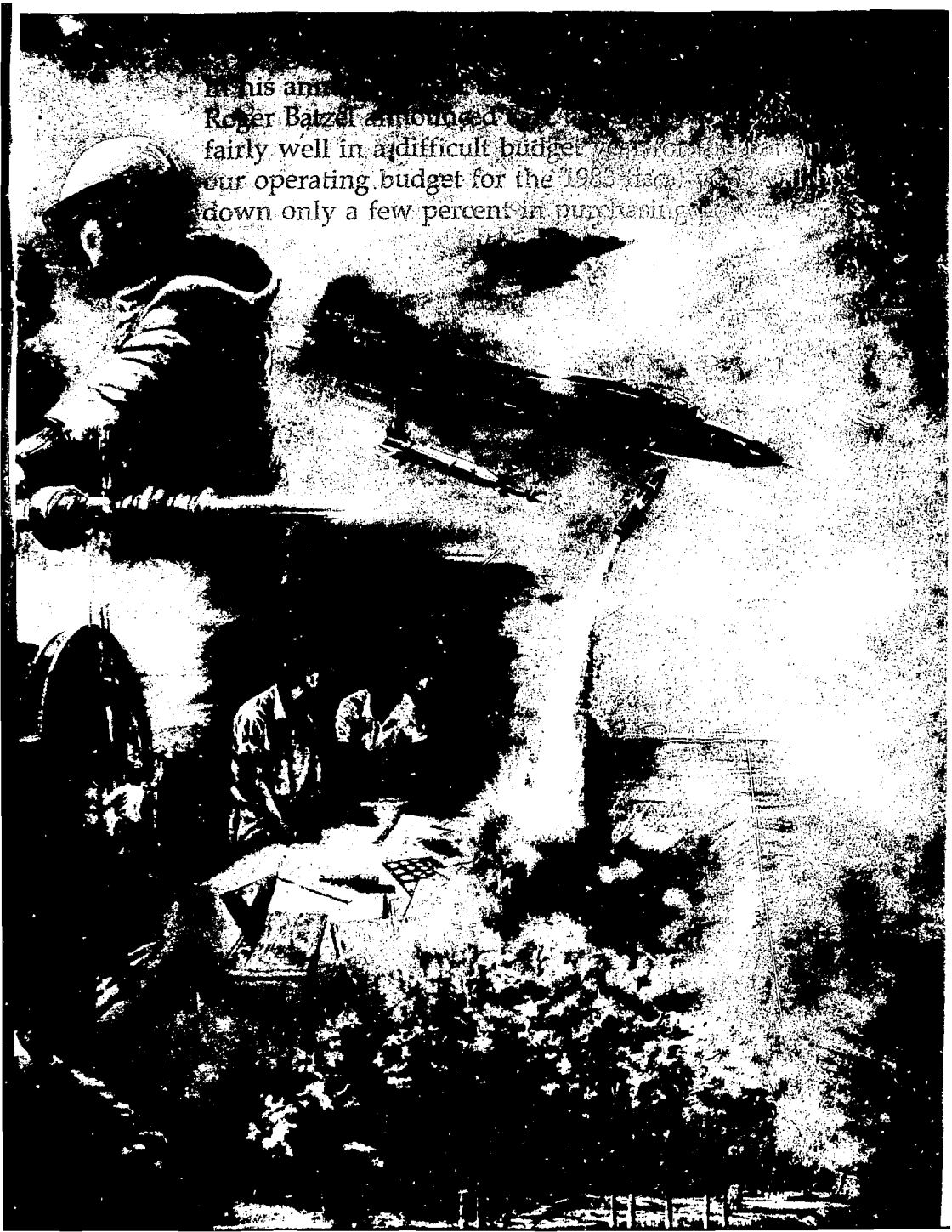

Director Roger Batzel presented his State of the Laboratory address on June 9, 1982, reporting a currently estimated $706 million total budget and a $515 million operating budget for fiscal year 1983. When the impact of inflation is taken into account, this represents a purchasing power almost equal to that of last year (see Tables 1 and 2). Batzel emphasized that these figures are subject to approval by Congress.

The largest single budget item from the Department of Energy (DOE) is for weapons research, embodying the biggest dollar increase in programmatic funding for the 1983 fiscal year. Inertial confinement fusion remains the second largest project at the Laboratory, with funding approximately equal to last year's. The overall laser isotope separation program will receive about the same dollar funding as in fiscal year 1982; magnetic fusion energy will receive a boost in funding that should almost offset the impact of inflation. This funding reflects the excellent technical results achieved by these two programs during the past year. Funding for most other Laboratory programs approximately equals that of fiscal year 1982, although some programs, notably those concerned with fossil fuel energy and with conservation and renewable energy, have been cut substantially.

Dr. Batzel commented on how some specific programs will fare under the proposed 1983 budget. Inflation will blunt most of the impact of the funding increase in the weapons program. He feels that the Laboratory's weapons effort remains undersupported and underfunded. Said Batzel, "We still do not have the level of support needed to meet our weaponization and advanced development commitments to the Federal government."

Batzel expressed satisfaction with the scientific achievements of the Laboratory's two laser isotope separation programs. Our program for the special isotope separation of plutonium made significant progress this year toward the achievement of its primary goals. The atomic vapor laser isotope separation (AVLIS) process for uranium, developed at LLNL, was recently chosen

over two other processes for full-scale development. Although funding for the uranium process of laser separation is down in fiscal year 1983, Batzel expects increased support in years to come.

The reduction in funding for the defense waste management program reflects a decision by the DOE to proceed with the borosilicate glass matrix rather than the LLNL-developed SYNROC for storage of defense nuclear wastes. However, support is continuing for our program in the use of SYNROC for commercial nuclear waste management.

The considerable funding decreases in our fossil fuel energy and conservation programs are the result, said Batzel, of Federal decisions to curtail government research in these areas. The administration believes that it is time for private industry to assume most of the responsibility for research and development in these technologies.

Dr. Batzel was gratified to see continued support for the Laboratory's magnetic fusion energy program. The program has demonstrated that the magnetic mirror approach to plasma confinement is definitely a viable option, and it should continue to be one of the two major thrusts in the nation's magnetic fusion effort.

The cuts in funding for the biomedical and environmental science programs for fiscal year 1983 reflect an administrative decision to "deemphasize" these areas. However, Batzel stated that it is his considered opinion that in the near future (perhaps as soon as 1984) there will be redress of these cuts and that funding will return to the 1982 level.

Regarding the liquefied gaseous fuels project, Batzel said that although much work is needed in this area—work that the Laboratory is well suited to perform—future funding is highly uncertain. Funding for reimbursable projects and work for others will remain about constant in terms of real dollars, the largest commitments being charged-particle-beam work and nonnuclear ordnance projects for the Department of Defense and licensing and safety studies of civil reactors for the

Table 1 Total LLNL financial activity, millions of dollars.

	Revised FY 1982	Estimated FY 1983
Operations	$480.5	$514.9
Equipment	36.7	43.7
General plant	5.9	5.0
Construction	139.3	142.8[a]
Total	$662.4	$706.4

[a]Represents an estimated $99.2 million in new funding and $43.6 million in funds carried forward from FY 1982.

Table 2 LLNL program funding, millions of dollars.

	Revised FY 1982		Estimated FY 1983	
Defense programs	$293.6		$325.3	
Weapons		210.0		236.4
Inertial confinement fusion		51.7		52.0
Verification and control		8.6		10.5
Safeguards and security		1.1		1.1
Isotope separation		19.6		25.1
Defense waste management		2.6		0.3
Fossil fuel energy	8.5		4.9	
Coal gasification and gas recovery		3.6		2.0
Oil shale		3.5		2.1
Gas stimulation		1.4		0.8
Conservation and renewable energy	4.2		2.7	
Solar technology and application		0.1		—
Transport energy conservation		0.3		0.3
Energy storage systems		3.5		2.4
Geothermal		0.3		—
Energy research	60.5		67.4	
Magnetic fusion		38.0		41.7
Magnetic fusion computer center		11.3		13.8
Energy sciences and nuclear physics		4.0		6.0
Health and environmental research		7.2		5.9
Nuclear energy	29.4		25.7	
Advanced isotope separation technology		24.5		20.0
Commercial nuclear waste		4.6		5.4
Conventional reactor system		0.3		0.3
Environmental protection, safety, and emergency preparedness	6.6		6.1	
Environmental activities		3.3		3.1
Liquefied gaseous fuel		3.3		3.0
Other work for the Department of Energy	15.1		12.3	
Reimbursable projects and work for others	62.6		70.5	
Total	$480.5		$514.9	

Table 3 LLNL reimbursable projects and work for others, millions of dollars.

	Revised FY 1982	Estimated FY 1983
Department of Defense	$36.6	$48.7
Nuclear Regulatory Commission	12.8	13.1
Department of Human Health Services	0.7	0.5
Environmental Protection Agency	3.3	3.0
Department of Transportation	0.6	0.5
Other Federal agencies	4.4	1.3
Non-Federal agencies	4.2	3.4
Total	$62.6	$70.5

Table 4 LLNL program manpower, full-time equivalents (FTEs).

	Revised FY 1982	Estimated FY 1983
Defense programs		
Weapons	3221	3193
Inertial confinement fusion	665	660
Verification and control	129	143
Safeguards and security	17	16
Isotope separation	222	213
Defense waste management	40	4
Fossil fuel energy		
Coal gasification and gas recovery	33	19
Oil shale	58	32
Gas stimulation	25	12
Conservation and renewable energy		
Transport energy conservation	10	9
Energy storage systems	28	21
Geothermal	1	—
Energy research		
Magnetic fusion	496	476
Magnetic fusion computer center	132	149
Energy sciences and nuclear physics	70	89
Health and environmental research	139	99
Nuclear energy		
Advanced isotope separation technology	312	295
Commercial nuclear waste	75	73
Conventional reactor system	5	5
Environmental protection, safety, and emergency preparedness		
Environmental activities	66	52
Liquefied gaseous fuel	58	43
Other work for the Department of Energy	196	153
Reimbursable projects and work for others	801	973
Total operations	6799	6729
Total construction and equipment	595	431
Total Laboratory	7394	7160

Nuclear Regulatory Commission (see Table 3).

Dr. Batzel noted that funding for construction at the Laboratory is promising, particularly for completion of the *Special Isotope Separation Facility*, for further construction of the Weapons Material Research and Development Facility, and for limited acquisition of land adjacent to the Laboratory. The funds proposed for the construction of the Nova laser facility and the Magnetic Fusion Test Facility-B are less than required to keep the programs on schedule, but, said Batzel, there is a possibility that Congress will approve additional funding.

In summary, Batzel noted that the Laboratory's overall budget is holding steady at a time when other federally funded institutions are suffering severe cutbacks. In terms of manpower, the hardest hit programs are those in fossil fuels and in conservation and renewable energy, which face cuts in FTEs of about 30% (see Table 4). However, we will be able to absorb these personnel in other Laboratory projects. The Laboratory as a whole must reduce its staff by about 250 persons to about 7000 by the end of fiscal year 1983. These reductions will be achieved via normal attrition, Batzel emphasized; with tight control on new hiring, we can avoid layoffs and begin the next fiscal year in a conservative and secure position. All things considered, Batzel said, we have fared pretty well, given the overall budget strictures facing the country.

Dr. Batzel then discussed some other issues facing the Laboratory. Regarding collective bargaining, he said that there probably will be an election for LLNL scientists and engineers some time this fall. He restated his belief that collective bargaining is not in the best interests of the Laboratory. Because we depend on technical expertise to conduct our programs, produce successful results, and thus obtain support for our work, anything that hinders this process, as he believes collective bargaining would, is detrimental to the Laboratory. We compete successfully with other research institutions, said Batzel,

because we are not only good, we are better than most. "If, for any reason, you lose the fine edge of technical excellence, you cannot compete." As illustrated by the selection of our AVLIS process, competition is playing an increasingly important role at the national laboratories.

Batzel also discussed demonstrations against LLNL, noting that much effort has been devoted to working out ways to protect Laboratory people and property and to developing plans to handle any potentially explosive situations that might arise. He stressed that it is imperative that Laboratory employees are not exposed to situations in which they might be injured. Said Batzel, we just cannot have any violence to or by Lab people; it would do great harm not only to the individuals but also to the Laboratory as a whole.

Regarding the demonstrators' protest against nuclear war, Batzel made the following statement: "There is general agreement that we want to avoid nuclear war and live in a peaceful world. The major argument centers around the way in which the country goes about maintaining peace in the world. As far as the U.S. is concerned, from the point of view of major worldwide conflict, we have avoided it, I believe, as a direct consequence of the fact that the U.S. has had a strong defensive military posture (a posture that must be maintained). Nuclear weapons are an important and integral part of our defensive structure, and we have a continuing and even increasing responsibility to the country to maintain this technology for the United States."

Dr. Batzel also mentioned that in this era of tight Federal funding and the scrutiny faced each year by every Laboratory project, we have been conducting an ongoing and comprehensive long-range planning effort. We are assessing the potential of new areas of research in terms of the country's future research needs and the Laboratory's capabilities and expertise. Batzel emphasized that such efforts are vital to the continued success of the Laboratory; after all, he said, "We cannot just sit still and wait and hope that somebody will take care of us; we are going to have to look after ourselves in this world."

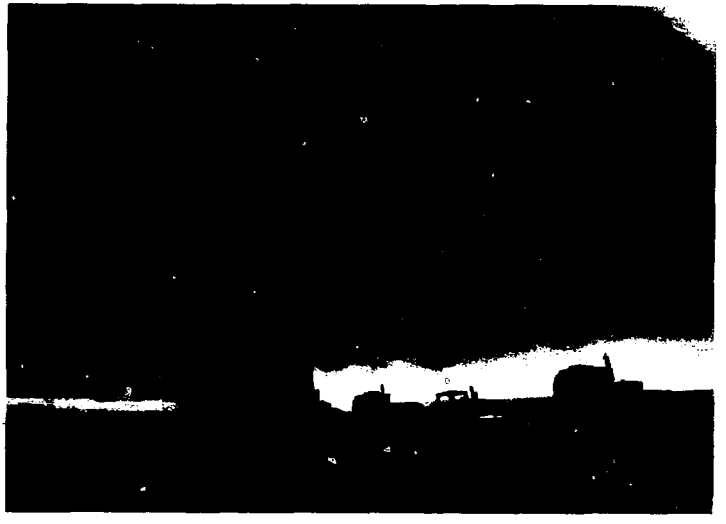

Ever since its founding thirty years ago, LLNL has been predominantly a nuclear weapons design laboratory. However, the expertise we have developed in performing this task has also proved valuable in other areas of defense research such as inertial confinement fusion, laser isotope separation, nonnuclear ordnance, and particle-beam technology. Our nuclear weapons, inertial-confinement fusion, and isotope separation programs are funded by the U.S. Department of Energy (DOE); our nonnuclear projects are conducted under the auspices of the Department of Defense (DOD).

DOE Programs

The Laboratory's nuclear weapons effort for the DOE involves three programs: nuclear design, nuclear testing, and military applications. The nuclear design program explores advanced weapons concepts and pursues research in weapons physics. The nuclear test program conducts device tests at the Nevada Test Site, designing, constructing, and fielding the downhole canister and diagnostic equipment. The military applications program is responsible for developing and maintaining a modern, reliable nuclear stockpile and for analyzing and evaluating the uses of nuclear weapons.

Nuclear Weapons Design

The trend in nuclear weapons design is toward smaller warheads with improved safety and security. The improved accuracy of the newer delivery systems makes it possible to achieve the same military effectiveness with a significantly reduced warhead yield and weight. Other nuclear design efforts include reducing the collateral damage of nuclear weapons and tailoring nuclear effects for specific purposes. It is also important to maintain an expertise in areas where potential new developments could significantly alter the status of the nuclear deterrent.

Table 1 Performance enhancements obtained with different versions of a representative two-dimensional hydrodynamics code.

Computer	Relative performance
CDC 7600	1.0
Original Cray 1	2.3
Vectorized Cray 1	4.3
Optimized Cray 1	8.0

Using Cray 1 computers for nuclear design. One of our principal tools in nuclear design is our high-speed computing system, which consists of seven large computers (four Cray 1s and three CDC 7600s) interconnected by the Octopus network. The Crays perform calculations in more efficient ways (by vectorization, for example) than the older 7600s. Since the first of the Crays arrived in 1979, we have been engaged in a program to convert our many design codes for operation on the Crays to reap the benefits of this increased efficiency.

Within the past year, we have finished converting about 20 of our major nuclear design code systems, representing roughly 1.5 million lines of code. In doing this, we used many of the latest software engineering developments to enhance the reliability, maintainability, documentation, and portability (the ability to move from one computer to another with minimal conversion) of our codes.

The actual performance improvement obtainable from this conversion depends, in each instance, on the numerical algorithms used and, among other variables, on the size of the problem. Table 1 gives the range of performance improvements obtainable, using as an example four different versions of a representative code.

Flash X-Ray facility. Another facet of our nuclear design effort is the testing of computer codes to see how closely they predict what will happen in a real implosion. To do this, we build full-scale (but nonnuclear) models of nuclear devices, detonate their high explosive, and take high-speed pictures of the explosion-implosion process. Because the vital components we wish to study are deep inside the model and

are surrounded by metal shells, the only practical way to obtain such pictures is with high-energy x rays.

To get a good picture of something moving fast, we must use a very brief x-ray flash. To get enough x rays through the device to form an image on the photographic plate, we must use very penetrating x rays and make the flash very bright.

We have been generating such x-ray pulses by accelerating intense beams of electrons to high energy and stopping them in a metal target. However, at this stage in our research, we need even clearer pictures than this equipment can provide. To meet this need, we designed an even more powerful electron linear accelerator for our Flash X-Ray (FXR) facility.

We recently finished building this 20-MeV high-current electron accelerator (Fig. 1) and are now in the process of testing and tuning it for operation. In preliminary measurements, the FXR has already produced close to the design dose of 500 R at 1 m in a 60-ns burst, even though it has not yet reached the design current of 4 kA. When this facility becomes operational later this year, it will be the most advanced hydrodiagnostic facility in the free world.

Nuclear Testing

Nuclear testing involves far more than just burying a device in a hole and detonating it. There are many scientific and engineering challenges, large and small, associated with the device design and the emplacement of a multi-tonne canister (containing the nuclear device and its associated diagnostics package) hundreds of metres below the surface. We must go to great lengths to guarantee the integrity of the mechanical and electronic systems of the test device and diagnostics as they are lowered into the emplacement hole. Furthermore, we must carefully backfill the hole to ensure the containment of radioactive debris underground after the device is detonated. There is also the problem of transmitting data, as the device explodes, from the diagnostics instruments to the recording equipment on the surface, all in minute fractions of a second. Once the device has been detonated, we must find ways of collecting and analyzing samples of the radioactive gas and solid debris from the explosion to determine how the device performed.

New cable emplacement system. We have found a way to make a substantial saving (about $2 million/y) in

Fig. 1

Recently finished 20-MeV high-current electron accelerator for the Flash X-Ray (FXR) facility. In preliminary measurements, this FXR accelerator has produced close to its design dose even though it has not yet reached its design current. When operational later this year, the FXR will be the most advanced hydrodiagnostic facility in the free world.

our nuclear testing effort by improving the efficiency with which we emplace the devices to be tested. We sometimes use as many as 200 cables to fire a device and transmit explosion diagnostic data to the recording instruments. While we lower the package containing the device and diagnostic canisters (anywhere from 200 to 700 m downhole), we must gather the cables into bundles and attach them at frequent intervals to the emplacement pipe to support them and to prevent stemming stresses (associated with backfilling the emplacement hole with sand and gravel) from breaking the cables. To prevent the formation of channels in these cable bundles, along which radioactive gases might travel after the nuclear explosion, we fan the cables apart from time to time to allow the stemming to sift in around each one.

All this manipulation involves many crafts and much hand labor, and it takes time. We have now built and tested a ten-cable demonstration module of a new computerized cable downhole emplacement system that will automatically control the tension on each diagnostic cable to just support the weight of that portion which is hanging in the hole (Fig. 2). Thus, each cable is supported independently from the ground surface, the stemming material can fill in around the cables without forming channels, and the device can be lowered by fewer workmen.

The chief advantage of this new cable downhole system, however, is speed. With the old system, at least 80% of the emplacement time is spent waiting for the various hand operations. With the new system, the device can be lowered almost continuously, reaching its proper depth in about two days instead of two weeks.

The new system may also make it possible to recover the emplacement pipe for reuse, allowing another large saving. This pipe is expensive; it is made of special steel and extensively pretested to make sure it is strong enough to support the device and diagnostic canisters (which can weigh hundreds of tonnes). In the old system, this pipe had to stay in the hole and be destroyed because all the diagnostic cables were connected to it. With the new system, we may be able to free it as soon as the stemming locks the

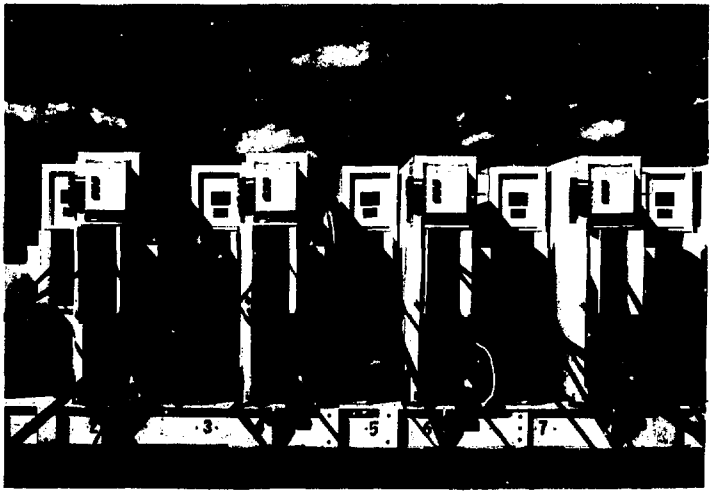

Fig. 2

Ten-cable demonstration module of our new computerized cable downhole emplacement system. This system automatically controls the tension on each diagnostic cable to just support the weight of that portion that is hanging in the emplacement hole. This cable downhole system allows us to lower the test device and diagnostics package using fewer workmen and in a fraction of the time previously required (two days instead of two weeks).

device canister in place and use the pipe over again.

Downhole refrigeration. To make sure that our nuclear weapons will function properly through the range of environmental conditions defined in the military specifications, we must be able to simulate these conditions underground during testing. We have long been able to maintain low humidity and high temperatures underground (electric heaters are easy to install, and the earth is an excellent insulator). However, maintaining the low temperatures for the long period required for some tests is a more challenging assignment.

We have developed a two-stage mechanical refrigeration system that can chill the device to $-54 \pm 2.8°C$. The refrigeration system is self-contained and includes a large volume of water as a circulating cooling medium for the system. The water serves as the heat sink for the heat extracted from the device and that generated by the mechanical equipment of the refrigeration system itself. At present, however, the system has a limited operating life; it quits when the water gets too hot. Therefore, for a longer lived refrigeration system, we enlarge the water tank (heat sink).

With additional development and testing, it might be possible to improve this downhole refrigeration system by circulating cooling water from the surface to obtain unlimited operating life. We might also add another stage of refrigeration for even lower temperatures. Neither of these improvements is required at present, however, because we can meet anticipated low-temperature requirements with our present design techniques.

Collecting nuclear test data with optical fibers. We are developing the use of optical fiber cables for improved diagnostic-data collection. The Fiber-Optic Research Experiment (FOREX) we installed in a recent nuclear test collected light from radiating materials near the nuclear device and transmitted it several hundred metres to a recording station located on the surface. These measurements provided new information about material properties at extreme temperatures and pressures.

Optical fiber cables are significantly smaller, lighter, and less expensive than coaxial cables. They also provide a faster response time than can be obtained with coaxial cables over comparable distances. We feed the output of these fiber-optic cables into a compact 30-channel streak camera, thereby replacing 30 oscilloscopes and saving space in the restricted quarters of the recording trailer. The result is a high-capacity, wide-bandwidth system that can be fielded at relatively low cost in manpower, equipment, space, and materials.

Sampling radioactive gases after a test. Another development to save time and improve accuracy in diagnosing device performance is our system for collecting and evaluating samples of radioactive gas from a nuclear explosion. One method of obtaining gas samples involves drilling back into the explosion debris, a process that is too slow to recover samples of short-lived radioisotopes. Our prompt gas-sampling system includes a pinch-off-proof tube that enables us to draw samples immediately. With a recently added, newly developed field mass spectrometer, we can now determine the chemical composition of the flowing sample gas. This enables us to make sure that only relevant samples are diverted for additional detailed analysis.

With this gas-sampling system, we were able to study the vexing problem of fractionation, that is, the possibility that some unknown underground process was changing the composition of the debris gas before we could sample it. Such studies are needed to help us determine how fractionation works and how to prevent or predict its effects.

In some of our experiments, we collected gas samples simultaneously from several locations in the debris column. Our measurements showed that fractionation can, indeed, change the ratio of heavy gases to light gases without changing the ratio of one light gas to another or of one heavy gas to another

Fig. 3

Direct evidence of gas fractionation in nuclear test rubble over a 43-day interval: data obtained with the prompt gas-sampling system (○) and by postshot drillback (△). (a) The helium-4 helium-3 ratio remains constant (light gases). (b) The xenon krypton ratio also remains relatively constant (heavy gases). (c) The krypton helium-3 ratio, however, varies over a wide range (heavy vs light). Fractionation has long been suspected, even without such direct evidence. We will now be able to study the causes of fractionation and either prevent it or compensate for its effects.

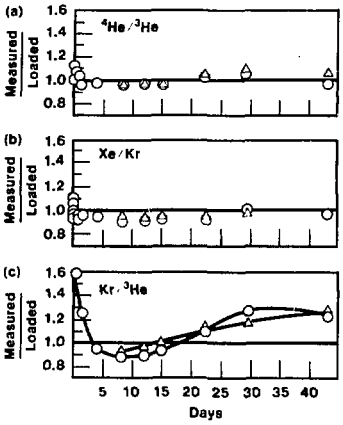

(Fig. 3). These results indicate that, until the fractionation phenomena are better understood, we should use helium-3 as a tracer for fusion-produced helium and krypton or xenon as a tracer for fission-produced gases.

Military Applications

The work of the military applications program is exceedingly diverse. It includes feasibility studies, development engineering, a bit of specialized production, and a planning and evaluation program.

Feasibility studies of new weapons. We are conducting feasibility studies of (1) a future nuclear warhead for an air-to-air missile (Phoenix) to defend carrier battle groups against cruise missiles launched by enemy aircraft, (2) a replacement nuclear warhead for the Air Force's air-to-ground short-range attack missile (SRAM) that would use insensitive high explosive for enhanced safety in handling and deployment, (3) a nuclear warhead that would be used as a replacement for three antisubmarine weapons systems (ASROC, SUBROC, and B57 depth bomb), and (4) a new ground-to-ground missile system for the Army capable of delivering conventional, chemical, and nuclear weapons beyond the ranges of cannon or tactical rocket systems. We continued a warhead feasibility study and preliminary warhead weaponization engineering work for the low-altitude defense (LoAD) system for protecting prime targets against ballistic missiles. We also began a feasibility study of a warhead for the new Trident D5 missile that will enable it to attack hardened targets.

Weapons in development. The LLNL warhead projects that are currently in development engineering are illustrated in Fig. 4. Each poses a unique challenge to the designers. The B83 strategic bomb must be structurally rugged because it must survive being dropped from a low-flying aircraft onto a hard, irregular target. The W82 artillery shell must be capable of withstanding the enormous stress of gun launching and must be similar in flight characteristics to a conventional round (so that the artillery can use nonnuclear shots to determine beforehand where the nuclear round will go). The W84 warhead for the Tomahawk ground-launched cruise missile must incorporate many recently developed safety and security features to make it acceptable for deployment in Europe. The MK 500 ballistic reentry vehicle, designed for the Trident submarine-launched D5 ballistic missile, must be able to survive the multiple stresses of launch, passage through water, ejection into air, and ignition, and still reach its target.

The W87 warhead for the advanced ballistic reentry vehicle, to be used in the MX missile, is the latest of our development engineering assignments. This will be the first strategic reentry vehicle to incorporate insensitive high explosive (IHE), an enhanced-safety detonator to minimize the chance of an accidental explosion, and a fire-resistant feature to prevent dispersal of the fissile material even if the IHE should burn. These features combine to provide a warhead that can meet safety requirements even for a mobile ICBM system, allowing a wide variety of basing options for the MX missile.

Present development schedules for the W87 warhead call for an unusually short development engineering phase.

The early shift from development engineering to production engineering is possible because we have been working with the Air Force and its contractor, AVCO Corporation, for the past two years. Even with this head start, however, it will take a sizable effort to obtain and evaluate the needed test information (making sure that the warhead and the combined warhead/reentry vehicle can withstand transportation handling, powered missile flight environments, reentry conditions, and hostile nuclear effects, for example) before making production commitments on long-lead-time items.

Other DOE Work

A number of other national-defense-related projects are also sponsored by the DOE. These include the inertial-confinement fusion (ICF) program and the laser isotope separation program. The DOE also supports our work on the regional seismic test network, which combines the latest electronic and communications technologies to obtain comprehensive earthquake data for both research and treaty verification.

Inertial Fusion

The energy of a modern nuclear weapon derives, to a large extent, from the energy of thermonuclear fusion. One way of producing and studying fusion in a confined environment is to use lasers to bring, in a very short time, a pellet of deuterium and tritium to the very high temperatures and densities at which the target nuclei will fuse. This technique, known as inertial confinement fusion, has potential for civil applications in producing electricity and for military applications directed toward studying nuclear phenomena and simulating nuclear weapon effects on military hardware without fielding an actual nuclear test.

Novette. During the past year, we designed and began to build Novette, a two-arm laser system for both laser and target experimentation. It is being assembled relatively inexpensively, in the Argus laser building, from Shiva and Argus parts, a special frame, and borrowed large-aperture Nova laser components. When completed later this year, Novette will deliver about 10 kJ of green laser light (0.527 μm) in pulses ranging in length from 1 to 40 ns. For shorter pulses (down to 20 ps), the focusable laser power will be more than 10 TW.

Novette is designed to provide a flexible test bed for a wide range of laser studies, for irradiating special targets to acquire weapons physics data, and to support the Nova target program. The dominant incentives for assembling Novette are to gain experience with the Nova hardware and to improve our understanding of target irradiations with green light at 10 kJ, a hundred times more energy than was available for previous short-wavelength target experiments. Experiments with Argus and Shiva indicate that substituting short-wavelength light for the infrared fundamental laser wavelength will improve the laser-target interaction and fuel compression by reducing detrimental nonlinear optical processes in the plasma.

Turning red light into green or blue light. Neodymium-glass lasers such as Nova have a fundamental wavelength of about 1.053 μm (in the near infrared). To produce green or blue light (0.527 and 0.351 μm, respectively) with such a laser system, we had to develop large-aperture frequency converters to double or triple the frequency. Properly aligned crystals of potassium dihydrogen phosphate (KDP) will perform the frequency conversion. However, the largest single crystals of KDP currently obtainable measure 27 by 27 cm, less than half the aperture of the 74-cm-diameter Nova beam.

To circumvent this difficulty, we have developed a way to assemble the crystals in an array to provide the necessary large aperture. To further reduce the cost of frequency conversion, we have devised a way to use the KDP crystals and lenses to generate and focus either of the shorter light wavelengths (0.527 or 0.351 μm). The

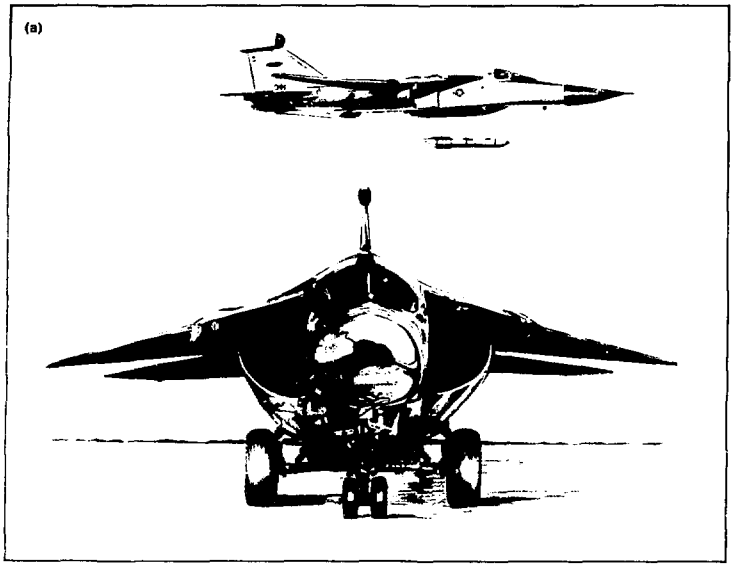

Fig. 4

LLNL warhead projects currently in development engineering. (a,c) The *B83, a modern strategic bomb* designed for parachute delivery from a low-flying aircraft (e.g., FB-111 or B-52), must survive impact, even on a hard irregular object, and detonate after the aircraft has had time to escape. (b) The Tomahawk ground-launched cruise missile. The W84 warhead for this missile incorporates many recently developed safety and

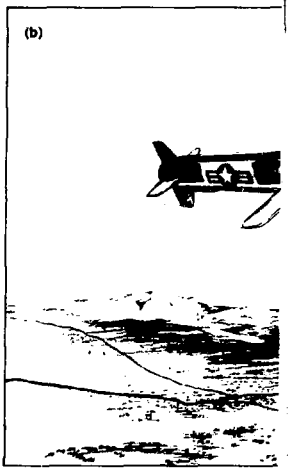

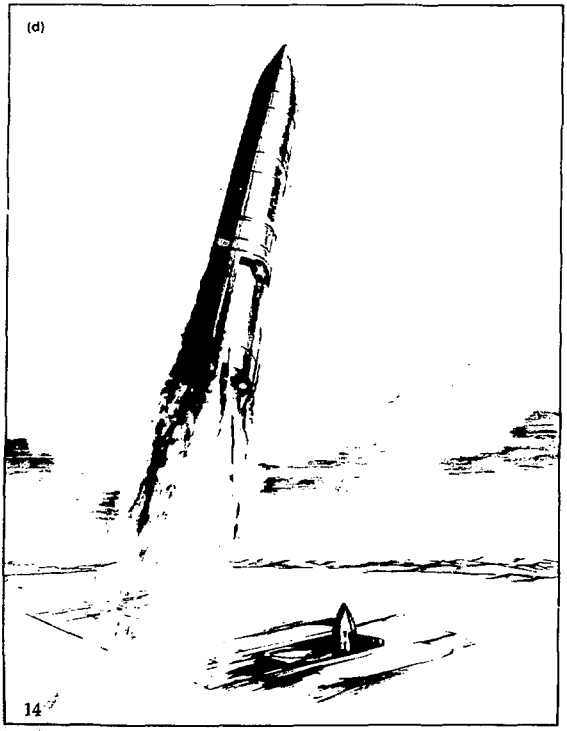

security features. (d) The W87 warhead for the MX missile will incorporate insensitive high explosive and fire-resistant components to minimize the possibility of plutonium dispersal in fires and accidents. (e) A 155-mm gun capable of firing a projectile armed with the W82 warhead. The W82 must withstand the extreme stresses of gun launching. (f) The MK 500 ballistic reentry vehicle, now in preengineering development, is designed for the Trident submarine-launched D5 ballistic missile.

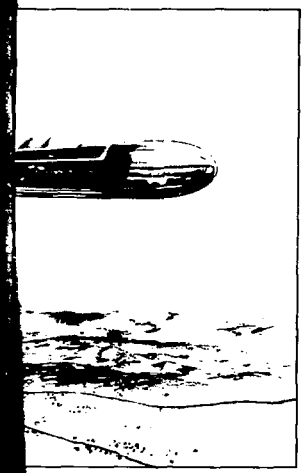

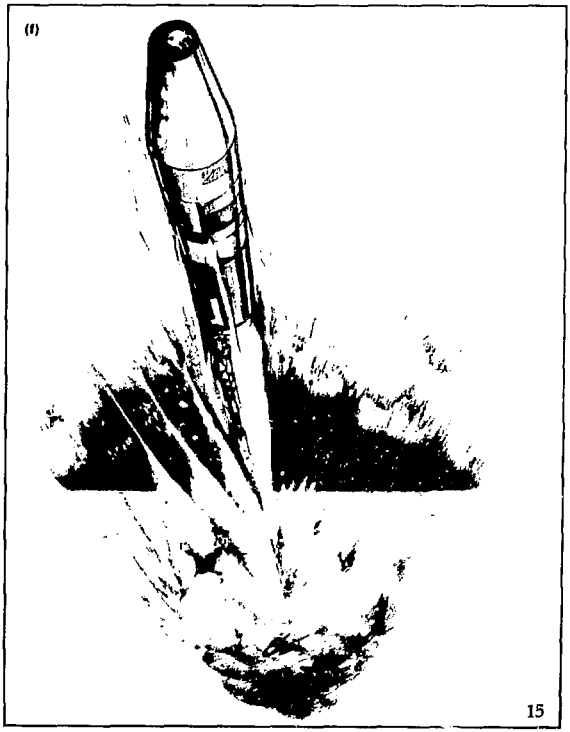

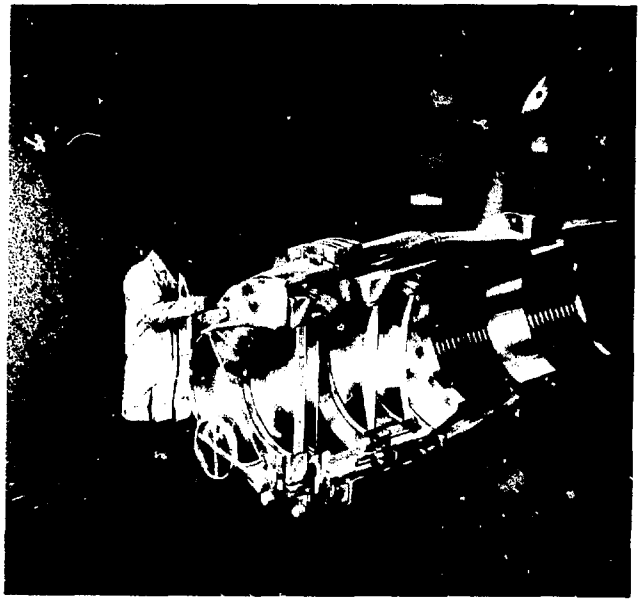

Fig. 5

Cut-away view of the large-aperture frequency converter (multilayer component in the foreground) for changing the infrared light from the Novette or Nova laser system into green or blue light for more efficient laser-target coupling in inertial-confinement fusion experiments.

cutaway drawing in Fig. 5 shows the size of the optical components; the frequency-converter crystal array and the multilayer element in the foreground.

Time-resolved x-ray imaging. Inertial fusion is, in many ways, a study in contrasts: huge machines amplify beams of light into brief pulses of energy, concentrating enormous power on microscopic targets. At the other end of the scale from the large frequency converter above, we have developed a time-resolved x-ray microscope with unprecedented spatial and temporal resolution to picture what happens in ICF targets under laser irradiation. With this equipment, we have measured accelerations of 35 Tm/s^2 and velocities of 120 km/s.

This x-ray microscope represents a remarkable feat of technology. X rays reflect from a metal surface only when they strike it very obliquely, at a grazing angle. For efficient reflection, the surface roughness must be less than 1 to 1.5 nm. For high resolution, the cylindrical mirror surface must conform to the ideal curvature within 3 nm over the several centimetres of its length, with slope errors of less than 5 μrad, and have curvature to better than 100 nm in a 2-cm radius. We have achieved these tolerances, using our diamond turning equipment and special polishing techniques, and have demonstrated a resolution of about 1 μm.

The x-ray microscope focuses its image, enlarged 22 times, on the slit of an ultrafast streak camera (also developed at LLNL), which records a slice of the image and sweeps it in time. The present version of this streak camera has a resolution of 150 μm, which produces a combined microscope/streak-camera resolution of 6 to 7 μm and a temporal resolution of 20 ps. The system images x rays ranging in energy from about 100 eV to more than 3.2 keV.

As an example of this instrument's capabilities, we conducted a joint experiment with the Naval Research Laboratory in which we investigated the ablative acceleration of matter. We used direct-drive laser irradiation under conditions approaching those anticipated for inertial-fusion-reactor targets. We irradiated an ultrathin carbon film (about 7 μm thick) with 10 of Shiva's 20 beams, overlapped to provide fairly uniform intensity over a 1-mm-diameter spot, in a 100-TW/cm^2 pulse lasting 3.5 ns. As the carbon ablated, it generated a pressure of 600 GPa and accelerated the foil at 30 Tm/s^2. Several nanoseconds later, the accelerated foil collided with a second foil of nearly equal mass, which then recoiled at nearly 100 km/s.

To backlight this violent action, we used the other 10 Shiva beams to produce a burst of 2.9-keV x rays from a palladium source. These beams were overlapped in a spot 800 μm in diameter for a concentrated intensity of 200 TW/cm^2. A beryllium shield 75 μm thick allowed the 2.9-keV x rays to pass through but protected the target foils from scattered laser light, soft x rays (less than 1 keV), and low-energy electrons (less than 50 keV).

Special Isotope Separation

Early in 1981, we undertook to demonstrate the technology of laser separation of plutonium isotopes. This effort includes several major activities:

- Construction of a 1-km evacuated beam tube 50 cm in diameter to carry light underground from the laser building to the plutonium building (Fig. 6).
- Construction of the optics and control elements required to maintain laser beam quality.
- Construction of an integrated plutonium-handling module to allow the vaporization, irradiation, separation, and collection of plutonium and its isotopes.

In addition, we have received support to construct a Special Isotope Separation Laboratory, now being built. This facility, scheduled for completion in 1983, will be used to demonstrate the equipment required for a full-scale plutonium-isotope-separation plant.

Seismic Verification of Test Treaties

The Regional Seismic Test Network (RSTN) is a prototype for the national seismic stations (NSS) that could be deployed in host countries under the terms of a comprehensive test ban treaty. The NSS form a network of broadband, digital, borehole seismometers and associated recording and transmission equipment that would be deployed at spacings of thousands of kilometres and would involve satellite telemetry of data in near real time.

The purposes of the NSS network include:

- Deterrence of evasive testing by restricting the locations and times at which it would be possible.
- Monitoring large areas and highlighting suspicious events, thereby making it possible for other national technical means, less well adapted to broad-area surveillance, to focus their attention on specific areas and times.
- Reducing false alarms by lowering the detection threshold, thereby assuring that the remaining unidentified events (there will always be unidentified events) will be below the range of suspicious events.
- Providing the host country with a set of common, verified data (that can be combined with data obtained from other stations within the host country) with which to mount a defense against a false charge of evasive testing.

The primary purpose of the RSTN is to provide a demonstration of the engineering readiness of the equipment and the seismological quality of the data necessary for in-country monitoring of a test ban treaty. The RSTN also provides an opportunity to carry out a number of other valuable tasks. For example, with the RSTN, it will be possible to demonstrate the verification capabilities of such a network using teleseismic techniques applied to regional data, and to determine the properties of regional seismic phases and relate them to the properties of the crust and upper mantle. This, in turn, will provide the understanding needed to permit prediction and rapid implementation of seismic monitoring stations in new locations. We will also be able to

Fig. 6

Construction of an evacuated beam tube 50 cm in diameter and 1 km long to carry light underground from the laser building to the plutonium building. This is part of our effort to demonstrate the feasibility of laser separation of plutonium isotopes.

use the RSTN to record nuclear explosions, analyze these data, and develop a catalog of well-characterized events that could be used as an historical basis for responding to challenges under present and future test ban treaties. In addition, the RSTN will make possible basic seismological studies of the mechanisms of intraplate earthquakes and of the structure of the North American continent.

As presently configured, the RSTN is a set of five unmanned, automated recording stations located throughout eastern North America and linked by geosynchronous satellite communications to a control station at Albuquerque, New Mexico. We specified much of the equipment that is being installed in the RSTN, and we are also participating in the data reduction and analysis for the system. Several criteria governed the selection of RSTN station sites. Stations had to be located in shield and/or platform tectonic provinces, and at least one station had to be within 1500 km of an intraplate seismic area such as the New Madrid region or the St. Lawrence-New England region. Station-to-station separations of less than about 3000 km were required. Also, there could be no nearby sources of seismic noise, such as heavy construction or heavy-vehicle traffic.

Each RSTN station consists of a seismometer package at the bottom of a borehole about 100 m deep, covered on the surface by a fiberglass dome containing the electronics equipment and an antenna for satellite transmission of the seismic data. The seismometer package contains two sets of three-component seismometers (a short-period set and broadband set covering frequencies from 0.01 to 10 Hz), a data authenticator to assure a tamper-proof system, and associated electronics. The dome also contains more electronics plus a generator to power the equipment.

Even though the RSTN is still in the shakedown phase of its development, there is generally good data transmission and acquisition. During a period of more than 4.6 Ms (about 1270 h), from November 27, 1981, to January 20, 1982, we achieved a data-acquisition success rate, for the entire chain from the station in South Dakota to the control center in Albuquerque, of about 97.5%. During this interval, there was one ten-day period of continuous operation without the loss of a single data bit.

It should be emphasized that the radiofrequency equipment was developed only a few months ago and is still being debugged. We expect the data-loss rate to decrease as equipment problems and operator interruptions decline during the shakedown period. In the months to come, as the RSTN system moves into full operation, the data-acquisition success rate should improve, more nearly approaching 100%.

DOD Projects

The Laboratory conducts selected projects for the Department of Defense. The expertise we have developed for the nuclear weapons program enables us to help the DOD improve the performance of nonnuclear weapons. Also, as a result of our fusion energy research, we have facilities and experience needed for charged-particle-beam research.

Nonnuclear Ordnance

Velocity-augmented munition. We successfully completed a flight test of the fuzing, deployment, and dispensing systems of the velocity-augmented munition (VAM). The VAM is a submunition we are developing to provide the medium-range air-to-surface missile (MRASM) with an effective tool for breaking up airfield runways. Each VAM contains three charges: a shaped charge in front to punch a hole in the concrete surface, a velocity augmentor to drive a main-charge projectile through the rubble left by the first charge to bury it under the runway where it explodes at some later time, forming a crater and disrupting an area of the runway. Each MRASM will carry about 40 VAMs, which will descend by parachute after launch.

We fired 18 VAMs (filled with mock explosive) from mortar tubes in a

modified wing tank of a T-33 jet aircraft flying at MRASM delivery altitudes and airspeeds. The tests showed that a mortar-tube launch is feasible under operational conditions and that the parachute will deliver the munition to the target with the proper angle of attack. We also proved that the safing, arming, and fuzing (SAF) system functions properly under these conditions.

To confirm the SAF results, we packed miniaturized, self-contained, shock-hardened data recorders on board several of the inert munitions. These recorders, designed to survive and function throughout the mortar-tube launch and target impact, used low-power solid-state memories to store the test data. They recorded the timing and event sequences within the SAF and parachute systems.

We are also adapting a new shock-hardened in-line SAF system, which we developed for Air Force modular weapons, as an alternate fuzing system for the VAM. To do this, we must pack about one third of the former energy-storage capacity in about one tenth the former volume. The new SAF system will contain a variable delay of up to several hours, providing a buried-mine capability to frustrate airfield damage-repair efforts. The time delay for each VAM would be programmed, just before launch, by an arming module aboard the missile.

Railgun. In collaboration with the Los Alamos National Laboratory, we have made significant progress in railgun technology during the past year, advancing from a single-use experimental device capable of launching only small plastic cubes to a multishot device capable of firing complex projectiles consisting of a plastic shell surrounding a metallic part (anything from a thin disk to a slender rod). Our railgun uses a plasma arc to accelerate the projectiles. This past year, we tested a variety of rail and rail-spacer materials to find a combination that successfully resists erosion by the plasma arc.

No explosively driven projectile can ever outrun the velocity of sound in the propulsive gas. Hence, the limiting muzzle velocity of a conventional rifle or cannon is on the order of 1 to 2 km/s, and of a two-stage light-gas gun is about 8 km/s. However, this limitation does not apply in the case of an electromagnetic launcher (like the railgun). This year, with our advanced railgun we demonstrated launch velocities of about 11 km/s and expect to exceed this with future designs.

To power the railgun, we experimented with two different sources, our 400-kJ capacitor bank and a magnetic flux compression generator provided by Los Alamos. The capacitor bank provided an average current of about 700 kA for a pulse length of about 250 μs; it was used mostly for development tests of round- and square-bore launchers for projectiles ranging in diameter from 8 to 24 mm and in mass from 2.8 to 93 g. The lightest of these was a tantalum disk 1 mm thick and 9 mm in diameter that reached a launch velocity of 2.9 km/s in a railgun only 40 cm long.

We used the magnetic flux compression generator to power a 12-mm-bore railgun 5 m long. The average current was about 700 kA, as with the capacitor bank, but the pulse lasted about twice as long (about 500 μs). With this equipment, we launched a tantalum disk similar to that mentioned above at about 11 km/s. Figure 7 is a color-enhanced shadowgraph of this projectile in flight, made with flash x-ray equipment; the timing data in this photograph enabled us to infer the projectile's velocity.

We have recently begun development work on a railgun specifically for equation-of-state research at extreme pressures. Our modeling applications frequently require us to extrapolate equation-of-state curves into the terapascal pressure range, but experimental limitations have prevented us from experimentally verifying these extrapolations. With an projectile impact velocity of 12 km/s, we could obtain pressures of more than 1 TPa in high-density targets, about twice the pressures attainable with projectiles from the two-stage light-gas gun.

Fig. 7

Short-pulse x-ray shadowgraph of a tantalum disk traveling in air at about 11 km s (more than 30 times the speed of sound) after leaving the muzzle of our 5-m-long electromagnetic railgun. (Color added by computer to enhance the visual contrast.) Originally 1 mm thick and 9 mm in diameter, the disk has been eroded by 4 m of flight through the air. Railguns offer the means to explore the states of matter at extreme pressures (around 1 TPa, about twice the pressure previously attainable experimentally).

Extrudable high explosives. Another recent contribution to weapons technology is our development of two new classes of high-energy extrudable explosives whose putty-like consistency allows them to be molded to precise shapes. Those in one class (extrusion cast explosives, or ECXs) contain a polymer system that hardens on curing; the others (paste extrudable explosives, or PEXs) obtain their system stability from a gelling agent.

These explosives are formulated from HMX and an energetic binder to achieve about 95% of the energy of LX-10. In addition to HMX, the main ingredient, each of our extrudable explosives contains about 25% of a 92/8 mixture of FEFO and a stabilizing agent. FEFO is a liquid explosive as energetic as nitroglycerin but much less sensitive and more stable. These new extrudable high explosives have several advantages over conventional plastic-bonded explosives (PBXs) of the same energy class:

- They can be formed at pressures of only 1.4 MPa instead of the 140 to 200 MPa needed for PBXs.
- They can be molded at room temperature rather than at the 80 to 120°C required by PBXs.
- They conform to the mold so closely that they require little or no machining to final form.
- They are less sensitive than conventional PBXs to mechanical stimuli.
- They are more uniform and homogeneous than PBXs.

To form an ECX, we blend all the ingredients in a high-shear vertical mixer until the consistency is very soft, about like that of toothpaste. We then deaerate it in a vacuum vessel to remove air bubbles and cast it under vacuum. The resulting castings are void-free to x radiography and are at 99.7% of the theoretical maximum density. Several variables in the polymer can be adjusted to change somewhat the mechanical properties of the finished product after curing.

After hardening, parts cast from an ECX can be handled and assembled like PBX parts. A PEX, on the other hand, will retain its plasticity indefinitely so that loading into the weapon may be delayed until just before use. This arrangement could reduce the damage caused by an accident in which the detonators of a weapon exploded; the PEX would be elsewhere in the system and would escape initiation.

Before we can design an adequate transfer mechanism to exploit the last-minute-fill option of PEXs, we will need to understand thoroughly the rheological properties of the PEX being used. For the formulations studied so far, the material's viscosity is high at low stress levels but becomes fairly low under high shear stress. This property keeps the material stable during storage but permits easy, rapid transfer when needed.

Advanced Test Accelerator

Construction work on our Advanced Test Accelerator (ATA) facility at Site 300 is on schedule for completion in October 1982. Designed to be the

world's most advanced high-intensity electron accelerator, the ATA, together with its associated program of experimental and theoretical physics, is the keystone of the Defense Advanced Research Projects Agency's particle-beam technology program. The ATA's primary purpose is to determine whether propagation of an intense electron beam through the air can be made stable and controllable and, if so, to answer questions about the potential military applications of such a beam.

During the past year, we have begun to install the accelerator and its associated power supply systems in the newly completed ATA building. When the ATA is finished, this system will have higher power and will pulse more rapidly than any comparable system in the U.S. So far, we have completed the installation of the main power system and the power conditioning equipment that shapes the short high-voltage pulses for the accelerator units (Fig. 8). To ensure reliability and acceptable component lifetimes, we extensively pretest all parts before they are installed.

The hierarchically organized network of mini- and microcomputers we will be using for control and monitoring of the ATA is a refinement and extension of the computer technology developed for the magnetic fusion program, with increased data-handling speed and capacity. Extensive on-line data processing and graphical display should expedite our bringing the ATA to full operational status during the 1983 fiscal year.

The most difficult technical problem in achieving the ATA's design goal of a 10-kA beam of 50-MeV electrons is to suppress potential radiofrequency instabilities (high-frequency oscillations of the beam about the accelerator axis) that arise from interactions between the high-current beam and the periodic structure of the accelerator. Such an instability, if uncontrolled, can amplify until it swings the beam aside into one of the accelerator modules or the wall of the experiment tank. One of our major research activities with the smaller Experimental Test Accelerator (ETA) has been to characterize and suppress these instabilities. The suppression techniques we have developed and demonstrated during the past year have enabled us to operate the ETA beyond its original design goal of 10 kA. We have incorporated these techniques into the ATA accelerator modules.

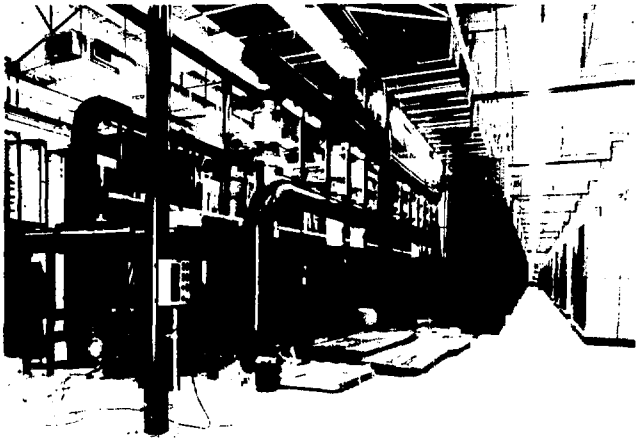

Fig. 8

Power-conditioning equipment being installed for the Advanced Test Accelerator (ATA), scheduled for completion this fall and for operation in the 1983 fiscal year. The ATA will explore the production of intense electron beams (10 kA of 50-MeV electrons) and the means for controlling and propagating them through the atmosphere.

In developing associated basic technology for future upgrades of the ATA, we have demonstrated a megawatt-class magnetic switch capable of operating at a rate of up to 10 MHz. These switches have ready application in such high-speed devices as electron-beam-pumped lasers, flash cine-radiography (x-ray motion picture equipment), and intense-beam accelerators. By extending this technology to the gigawatt, kilohertz range of the ATA, we should recoup capital costs with operating savings within a few years while greatly improving accelerator performance and reliability.

Key Words: Advanced Test Accelerator (ATA); atomic vapor laser isotope separation (AVLIS); beam weapons; cable downhole emplacement system; Cray 1 computer; downhole refrigeration; Flash X-Ray facility (FXR); FOREX; gas-sampling diagnostics; inertial confinement fusion (ICF); laser fusion; Novette laser system; optical fiber; railgun; regional seismic test network (RSTN); velocity-augmented munition (VAM).

Energy and the Environment

...s applying its unique scientific and engineering resources to the dual challenge of meeting future energy needs while maintaining the quality of the biosphere.

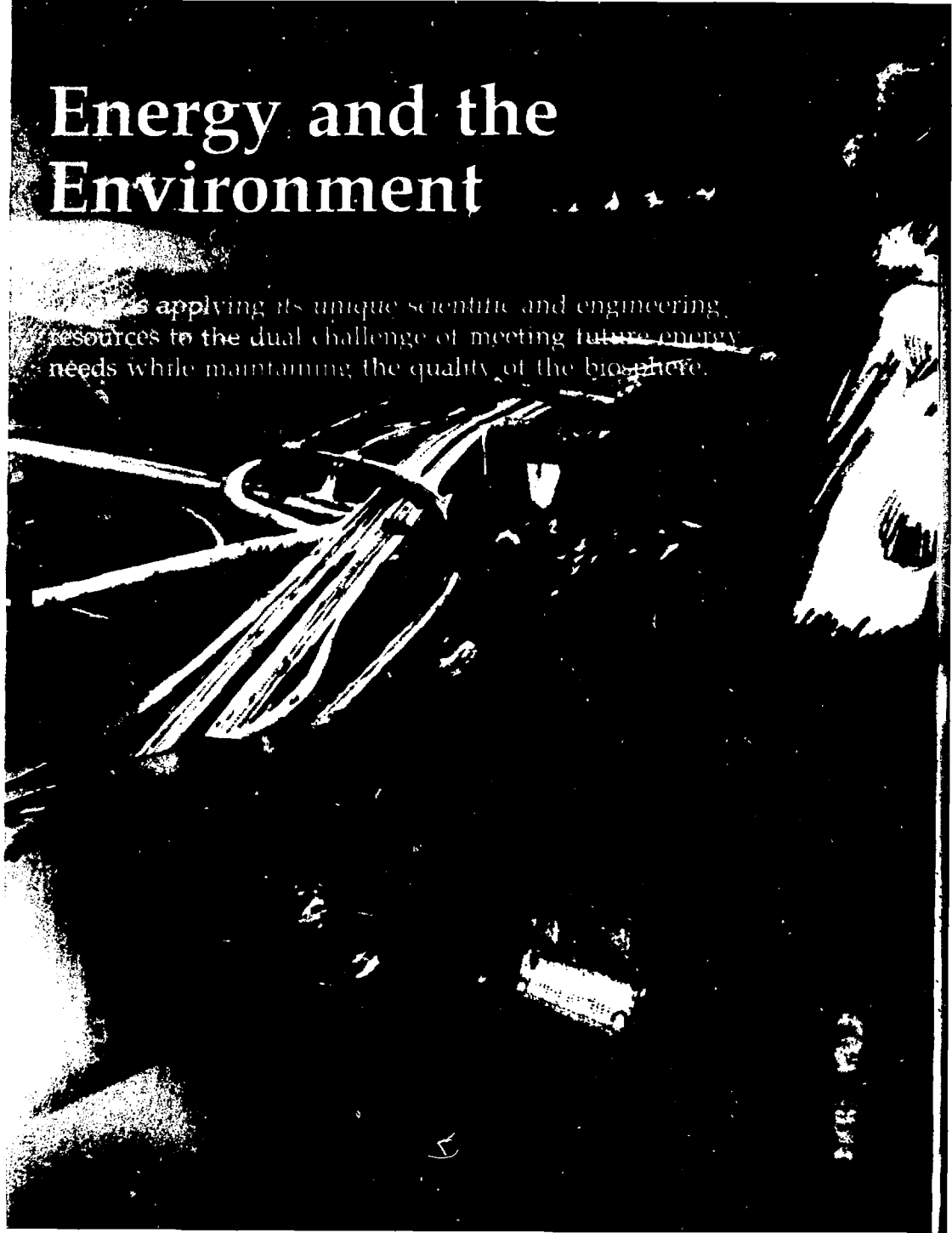

Our nation's success in coupling continued economic growth with environmental protection will require, among other things, the availability of abundant and nonpolluting sources of energy. Developing the technologies to resolve this multifaceted problem is a complex and lengthy process involving many disciplines. The largest of the Laboratory's energy projects seek to harness the energy generated by thermonuclear fusion. One avenue to this goal is magnetic confinement fusion, which uses a powerful magnetic field to confine a hot gas. Our magnetic fusion energy program recorded several important achievements during the past year. The Tandem Mirror Experiment Upgrade was completed on schedule and will soon begin experiments that will guide planning for the operating parameters of the large tandem-mirror MFTF-B machine. Our Mirror Fusion Test Facility project successfully completed a series of technology demonstration tests to verify hardware and software technology for the MFTF-B machine, including operation of the superconducting yin-yang magnet system. During this time, we also tested the facility's computerized control and diagnostics system.

We are applying laser technology to the complex task of separating one isotope of an element from other isotopes of that same element. Our atomic vapor laser isotope separation process, developed on a laboratory scale for the separation of uranium isotopes, was selected recently by the DOE for large-scale engineering development.

We are also developing high-performance electric battery cells that eventually could power the nation's fleet of motor vehicles. In addition, this country's substantial coal reserves are an important energy resource; we are experimenting with techniques to produce, *in situ*, clean gaseous fuels from coal deposits.

To ensure the safe, long-term storage of radioactive wastes, we are developing synthetic materials for immobilizing liquefied radioactive wastes in a form suitable for underground storage.

Another potential hazard to the biosphere is the increasing global level of atmospheric carbon dioxide; we have developed a highly accurate sensor that allows us to measure the carbon dioxide flux in remote areas. Because the worldwide transport and storage of liquefied gaseous fuels raises complex safety issues, we are conducting computer modeling studies and field experiments to better understand spill behavior and combustion physics.

The effects of biological cell damage caused by chemical and radiological agents in the environment are another source of concern. Our biomedical studies are aimed at a better understanding of the mechanisms of cellular change and the efficient identification of potentially damaging agents. These include studies of morphological changes in sperm cells, of processes that repair damage in genes, and of chromosome changes caused by damage to a cell's DNA. We have also developed techniques for quickly screening mutagens.

Magnetic Fusion Energy

The Laboratory's magnetic fusion energy (MFE) program is developing technologies that could unlock virtually unlimited resources to help meet the nation's energy needs. When two light nuclei combine, large amounts of energy are released. Creating the conditions to trigger and extract useful energy from this process is a complex and exacting technical problem. In our MFE program, we use intense, specially shaped magnetic fields to confine a plasma (a hot, ionized gas) while heating it to the high temperatures necessary to ignite a fusion reaction. (Progress in inertial confinement fusion, another approach to this source of energy, is reviewed on p. 13 of this issue.)

TMX Upgrade

Our Tandem Mirror Experiment (TMX) was operated from late in 1978 to early in September 1980, when it was shut down and disassembled. During its roughly two years of operation,

the TMX yielded a wealth of invaluable physics information, confining the hot plasma better than previous devices and confirming our theoretical predictions.[1] On the basis of our experimental results and theoretical insights, we developed a more advanced design—the TMX Upgrade—to extend and refine the knowledge gained from the TMX.

During 1981, we enlarged the existing facility to house the TMX Upgrade, completed fabrication of machine components such as magnets and tanks, and finished assembly and installation. Only 17 months elapsed from the time the DOE authorized construction to completion of the machine. The TMX Upgrade was built at its original budget of $14.5 million.

The TMX Upgrade incorporates two new features of our tandem mirror program: thermal barriers in the end cells and injection of neutral beams at several oblique angles (Fig. 1). The thermal barriers isolate the electrons in the end cells from those in the central cell, making it possible to heat them independently with microwaves. This innovation should produce a large potential gradient in the end plugs using lower magnetic fields and neutral-beam energies. The TMX Upgrade is also designed to use beam injection angles as an experimental parameter. We expect angles other than 90 deg to produce a plasma with improved microstability.

The neutral beams, consisting of energetic hydrogen atoms, deliver 10 MW of power at 20 kV distributed over 24 beams to heat plasma in the end-plug regions. Beams can be aimed at the plasma in several combinations of angles: 18, 45, 59, 65, 70, or 90 deg. We can apply another 800 kW of power to the plasma by heating it with microwaves generated by four gyrotrons at 28 GHz.

The water-cooled copper magnets in the TMX Upgrade produce the same 20-kG peak fields generated by the TMX. In the Upgrade, however, the magnet set is 14.2 m long, 50% longer than in the TMX, and the magnets have a larger inner diameter (40 cm in the end cells and up to 60 cm in the central cell) to accommodate a larger diameter plasma. The new magnet system comprises 24 magnets connected in 17 separately controlled circuits. The field is generated by 24 MW of dc power. Because of its greater length and diameter, the magnet system weighs 100 tonne, twice as much as in the TMX.

The vacuum chamber that houses the entire apparatus contains surfaces that pump out cold hydrogen gas, which would contaminate the plasma. The 540 m^2 of surface in the TMX Upgrade are covered with titanium atoms (sublimated from hot titanium wires) and are cooled with liquid nitrogen. These surfaces can pump hydrogen gas at a rate of 6×10^4 m^3/s.

Our first experiments with the TMX Upgrade will investigate the microstability of the plasma in the new geometry. Later work will study the generation of the thermal barriers in the end cells. The results of these

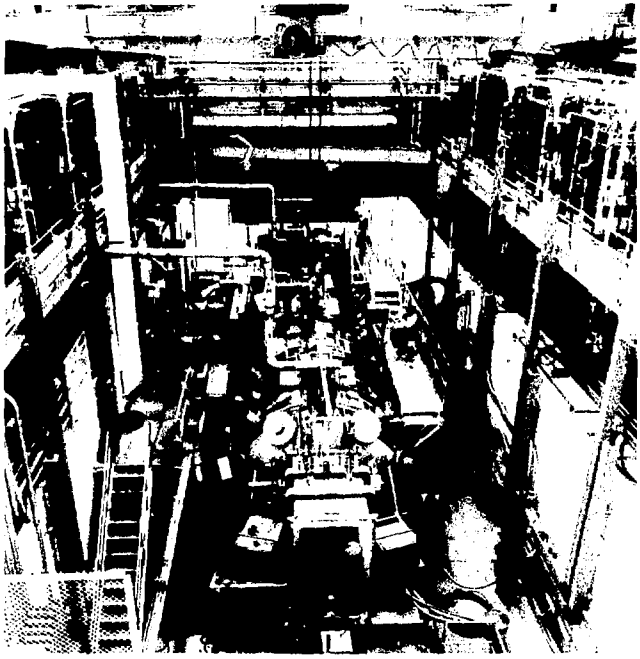

Fig. 1

The TMX Upgrade, which features a thermal barrier in the end cells and injection of neutral beams into the end plugs at various oblique angles. The thermal barrier isolates end-cell electrons from those in the central cell and makes it possible to use microwaves to heat them independently. This produces the necessary end-plug potential gradient without a large density gradient, reducing the magnetic field and neutral-beam energy requirements. In addition, oblique injection of the neutral beams is expected to improve the microstability of the plasma. The overall length of the machine is 22 m.

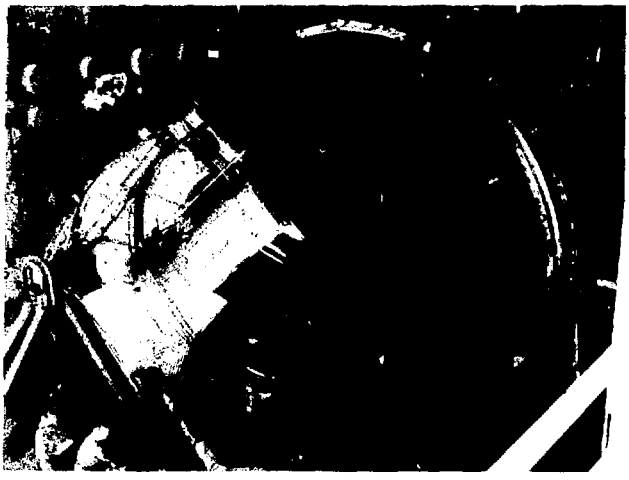

Fig. 2

One of the two yin-yang magnets in the tandem-mirror MFTF-B machine, shown during installation. The metallic covering is the liquid-nitrogen heat shield, cryogenically cooled with liquid helium, required to insulate the magnet against heat loss.

experiments will guide us in planning the operating parameters of the MFTF-B machine.

MFTF-B Technology Demonstration Tests

During 1981, the Mirror Fusion Test Facility (MFTF) project successfully completed a series of technology demonstration tests. Using original MFTF elements, the tests verified the technology for the hardware and software to complete the large tandem-mirror MFTF-B machine, scheduled for startup in late 1985.[2] Three technical milestones highlighted the test series. First, we operated the superconducting yin-yang magnet system (Fig. 2) at a current of 5775 A, its design level. The superconducting magnet performed as expected, with all peak fields, case stresses, and conductor strains accurately meeting predicted values. The 341-tonne two-coil magnet operated at full design level less than eight days after power was first applied. We also verified the design of the external vacuum system, the cryogenic system, cryopanels, controls, and plasma diagnostics. Cryogenic pumping tests fully confirmed the design-base vacuum pressure of 1.064 μPa. All vacuum and cryogenic subsystems tested leak-free under thermal shock, and pumping speeds for the external vacuum system were verified.

During the technology demonstration tests, we also began (and completed early in 1982) tests of the MFTF computerized Control and Diagnostics System (CDS), to be expanded for use with the larger MFTF-B. This control system embodies a hierarchical computer structure that enables us to collect, communicate, process, and display information at the appropriate stages of an experimental cycle. The CDS monitors and controls preparations for an MFTF experimental shot (up to one every 5 min during two 8-h shifts per day), maintains the operating environment during the experiment, synchronizes test events, monitors instrumentation, acquires diagnostic data on performance, and controls the complex procedures necessary to prepare the machine for maintenance during the shift following a series of experimental plasma shots.

The control system actually comprises two distinct but interacting systems: the Supervisory Control and Diagnostics System (SCDS) and the Local Control and Instrumentation System (LCIS). The LCIS provides interfaces between the operating/monitoring equipment and the SCDS, transmitting and translating data and control signals between the SCDS and each major operating and monitoring point.

During initial operation, the CDS operated the magnet system, the vacuum vessel, the external vacuum system, cryopanels, and the cryogenic system of the MFTF-B. We used the color displays and touch panels to control this integrated set of systems hardware. Data were transferred from consoles to local computers and thence to operating points through the fiber-optics links. Our hierarchical control system demonstrated the hardware and software capabilities necessary to operate the MFTF-B facility.

Initial operation confirmed the general architecture and design of both the SCDS and LCIS portions of the control

system. Although some problems occurred, we rectified most without difficulty. Some of our solutions took advantage of the system's data-rerouting capability. A more serious problem was memory crowding in the SCDS. In certain circumstances, this caused longer response times and occasionally blocked control functions. It is now clear that the CDS memory needs upgrading to accommodate the systems added for MFTF-B. To this end, we are expanding memory and increasing processor speed with improved equipment that is compatible with our existing software.

Laser Isotope Separation

Lasers can be used for the complex process of separating one isotope of an element from another isotope of the same element. The elemental metal is first melted and then vaporized to form an atomic vapor stream. The vapor stream is illuminated by laser light of a previously selected, precisely tuned wavelength. The atoms of the desired isotope absorb the laser light and are excited, but the atoms of the undesired isotope do not. By absorbing more laser light, the now-excited atoms become ionized and are deflected by an electromagnetic field into the product collector. The uncharged atoms pass through the collecting section and into the tails collector.

In April of this year, the atomic vapor laser isotope separation (AVLIS) process, which we have been developing on a laboratory scale for the separation of uranium isotopes, was selected by the DOE from among several competitors for large-scale engineering development. To bring our process to this point, we had to demonstrate:

- A mass balance between product and tails, showing consistent process physics and reliable operation of the fully integrated laser and atomic vapor system.
- A laser-system availability of at least 50% over weeks of operating time.
- A scaled-up atomic vapor system capable of producing high-quality uranium vapor.
- High-throughput materials handling for extended operating times.

With this selection of the AVLIS process, we are proceeding with large-scale engineering development and demonstration of the process in a pilot facility. Completion of this pilot program will provide a firm basis for building a uranium-isotope-separation production plant that should be able to produce nuclear fuel at a fraction of its present cost.

The Aluminum-Air Power Cell

Current supply uncertainties in imported petroleum and the prospect of a long-term decline in world petroleum production have stimulated the search for alternative fuels and technologies to power the nation's fleet of motor vehicles. To capture an appreciable share of the automotive market, an alternative power source must both compete economically with the internal combustion engine and roughly match its performance with regard to range, acceleration, and rapid refueling.

An electrically powered vehicle is a popular candidate for this application. Until recently, however, most battery technologies have suffered from cost, performance, or technical limits on their general-purpose utility. LLNL is the lead laboratory for DOE development of metal-air batteries. Our aluminum-air power cell is a key element in that program.[3] Now under development, this technology has the potential to satisfy performance requirements at a cost that should eventually compete with the rising price of carbonaceous fuels. Our role is to provide technical direction for the project and to conduct research in areas critical to integrating the diverse technologies it embodies. Much of the development work is carried out by industrial subcontractors with unique expertise in specific problem areas.

The promise of the aluminum-air power cell lies in its high energy-to-weight ratio (potentially more than 300 Wh/kg, nearly an order of magnitude greater than that of the lead-acid

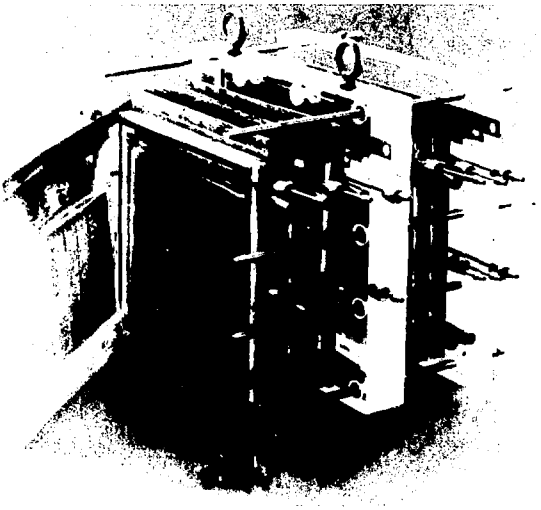

Fig. 3

Refuelable, multicell aluminum-air power module. Water and atmospheric oxygen react with aluminum anodes in the stack to yield electrical energy and a reaction product. In an operating vehicle, the aluminum anodes must be replaced periodically. Last year, we successfully tested this subscale design. Further development eventually will decide the technical and economic feasibility of this technology as a long-term replacement for the internal combustion engine in motor vehicles.

battery) and its refueling convenience (fresh reactants—aluminum and tapwater—can be added in about 15 min). The major component of the cell is its refuelable cell stack, in which the energy-producing reaction takes place (Fig. 3). Water and atmospheric oxygen react with aluminum anodes in the stack to yield electrical energy and a reaction product called hydrargillite (aluminum trihydroxide). The aluminum anodes must be replaced periodically. A cell stack large enough to power a vehicle will contain about 60 replaceable cells electrically connected in series, each with a working area of about 0.1 m^2.

Our development and testing program is progressing, step by step, toward its ultimate goal of vehicle-size batteries. Beginning with subscale single cells, we proceeded to full-size single cells and then to subscale, rapidly refuelable single cells. Last year, a subcontractor successfully tested a full-size (0.1-m^2), rapidly refuelable single cell. Our major achievement in 1981 was the testing of a subscale, rapidly refuelable multicell design at LLNL. These were the first tests of an aluminum-air multicell that reflected vehicle requirements with respect to air and electrolyte flow, electrical connections, refuelability, and operating conditions. Measurements of changing electrolyte composition were an important part of the tests, since this composition varies as the aluminum anode is consumed.

The multicell design consisted of six 167-cm^2 cells electrically connected in series. Electrolytes flowed in two parallel circuits though a series of three cells. We conducted two separate tests over a total operating period of 8.5 h. We measured the polarization characteristics of each cell at 60 and 70°C under extreme conditions of current density, electrolyte composition, and air and electrolyte flow rates. Our computerized data acquisition system recorded 25 test parameters every 30 s.

The results showed that peak power was 18% greater than in our previous 25-cm^2 single-cell baseline measurements. Most of this improvement may be attributed to the fact that air had better access to reaction sites within the air electrode, resulting in lower voltage losses at high rates of discharge. We found that peak cell power declined as the dissolving aluminum anode produced an increased concentration of sodium aluminate in the electrolyte. However, this effect can be mitigated by allowing cell temperature to track the concentration change. We also learned that shunt currents through the electrolyte connections do not degrade cell performance and cause only negligible power losses.

Our next step in the program will be to integrate a full-scale multicell stack with a crystallizer unit (which controls electrolyte composition) and a means of controlling electrolyte temperature. We will investigate the behavior of this system over the range of operating temperatures and electrolyte composition anticipated for a vehicle's operating and shutdown modes.

There remain some challenging problems to solve before we can fully establish the economic and technical feasibility of the aluminum-air power cell.

However, this year's progress suggests that the aluminum-air battery is a leading candidate for a long-term replacement for the internal combustion engine.

Large-Block Coal Gasification Experiments

Underground coal gasification may be the key to recovering much of the energy in the one-half of our coal deposits that lie too deep beneath the surface to be mined economically. In this technique, coal deposits are burned *in situ* to produce combustible gases that can then be extracted and used as fuel. To support the burning, oxygen and steam are pumped through injection holes drilled from the surface down to the coal seam. The product gases are piped up to the surface through other holes. For several years, we have been conducting field experiments for the DOE to investigate more effective and economical methods of exploiting this technology.[4]

The controlled retraction of the injection point (CRIP) technique of coal gasification was devised in response to the finding that the gases generated by *in situ* burning lose heat to inert roof materials as the burn cavity expands.[5] When coal dries, it shrinks, crumbling and collapsing faster than it is consumed by the oxygen. Gasification thus occurs in a packed bed of coal around the injection point. This situation produces gas of a consistently high quality until the roof rock falls in and the bed of coal rubble is consumed. At this point, heat losses to the inert roof material become a significant drain on the energy available from combustion, and the heating value of the gases begins to fall, becoming uneconomic.

With CRIP, we move the burn zone back into fresh coal by deliberately destroying a section of the injection pipe. In early 1981, we completed a series of five large-block gasification experiments designed to investigate the effect of the steam-oxygen injection ratio and flow rate on the shape of the burn cavity. The last of these tested the CRIP concept.

Fig. 4

Cross-sectional photograph of the excavated burn cavity after experiment No. 5, conducted at the Widco mine in Centralia, Washington. The view is at a point near the end of the injection pipe. Grid spacing is 1 m. The injection channel, lined with slag and ash, is the white-circled area at the bottom center of the grid. The top quarter of the burn cavity is open, and the lower three quarters are filled with char and ash. The extent of the char zone is outlined in red; the altered zone lies between the char zone and the outer area marked in white.

The experiments were conducted at the Widco mine near Centralia, Washington. In each, we drilled down an inclined seam at an exposed coal face. We used a vertical well to observe visually the burn cavity and measure its temperature. Our plan called for burning about 25 m^3 of coal for each test, measuring the composition of the product gases, and observing burn-cavity shapes by excavating afterward.

We found that variations in the steam-oxygen ratio (from 1:1 to 3:1) and flow rate had little effect on the composition of the product gases. Gas quality was consistently high, averaging 244 kJ/mol in all cases. Burn-cavity shapes were gratifyingly similar to those produced in our small-scale laboratory experiments. All exhibited the same oval cross section and all were partly filled with coal rubble and char (Fig. 4).

The last experiment was designed to test the CRIP technique by starting a new burn zone in fresh coal (Fig. 5). The CRIP test lasted four days. After burning the first cavity for three days, we used a pyrophoric, silane-ignited propane torch to cut off a 7-m section of the stainless steel injection pipe. At this point, we established a cavity at the new position. The second cavity burned for 24 h, demonstrating the validity of CRIP as a means of enhancing gas production.

Encouraged by these results, we are proposing a new series of tests to further develop the CRIP technique. The

Fig. 5

Artist's conception of the CRIP test. The first cavity was allowed to burn for three days. A 7-m section of the injection pipe was then cut off with a silane-ignited torch and a new burn cavity started at that point. Real-time thermocouple data and post-burn observations verified the success of the CRIP technique.

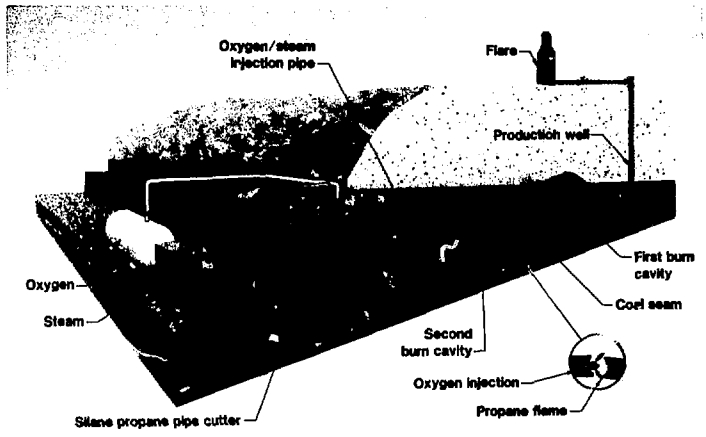

first of these, called the partial-seam CRIP test, will use half the thickness of the coal seam and will allow for four or five withdrawals of the injection point during a 30-day burn period. In contrast to earlier tests, we will install the production channel above the injection channel. As the burn progresses, the coal beneath the production channel will collapse. This should prevent the slag from the high-ash (14%) coal from plugging the channel and ensure a continuous gas connection with little pressure drop. This geometry is also the simplest to link with a vertical well.

Our second proposed test is a full-thickness 90-day burn, which will enable us to experiment with gas utilization. If successful, we will construct a small commercial-scale system by drilling additional holes, cleaning up the gas, and building a pipeline to a nearby power plant, where the gas will be used as a supplementary boiler fuel. Preliminary cost estimates for such a system give a price of about $1.42/GJ for raw, medium-Btu gas, making it economically competitive in this application.

SYNROC Storage of Radioactive Wastes

The permanent disposal of high-level reactor waste is of major import today. The SYNROC project at LLNL is concerned with the form in which liquefied radioactive wastes are stored.[6] Reprocessed wastes from reactor fuel consist of liquids and semisolid sludges of various materials. In this country, such wastes result from defense activities, including naval propulsion reactors and the production of plutonium and tritium for nuclear weapons, and from commercial power reactors.

Current plans call for immobilizing these wastes in borosilicate glass and eventually disposing of this glass in an underground repository. Although the process engineering of borosilicate glass is well advanced, its performance properties are poorer than those of several newly proposed alternatives. One of these is SYNROC (synthetic rock). SYNROC was conceived in 1978 by A. E. Ringwood of the Australian National University as a medium for disposing of wastes from commercial nuclear power reactors.[7] In 1981, the DOE chose SYNROC from among eight other candidates as the most promising alternative to borosilicate glass for the permanent storage of high-level defense wastes. The current goal of our project is to extend SYNROC technology to demonstrate its potential for large-scale production.[8] We are also evaluating the potential cost savings

from using better waste forms such as SYNROC.

We have found that laboratory-synthesized samples of SYNROC immobilize the long-lived radioactive wastes—primarily the actinides and rare earths—up to 1000 times more efficiently than borosilicate glass. (More specifically, the amount of these elements deposited in solution from SYNROC samples subjected to leach tests was up to 1000 times less than for borosilicate glass.)

SYNROC's composition borrows heavily from nature. Its suite of minerals was intended to mimic crustal rock with long-term stability that contains waste-like elements. The SYNROC host minerals for wastes, all having analogues found in nature, are zirconolite, perovskite, and hollandite. Zirconolite and perovskite have retained radioactive elements such as uranium and thorium in their crystal structure for as long as 500 million years.

The synthesis of SYNROC is straightforward. We combine TiO_2, ZrO_2, CaO, and Al_2O_3 with an aqueous slurry of simulated Savannah River Plant wastes and blend the mixture. The slurry is spray dried at 125 to 150°C, at rates up to 10 kg/day. The dry powder is then decomposed (calcined) at 650°C in an Inconel rotary furnace. Finally, we either hot press the resulting material in a graphite die assembly for 1 h at about 14 to 28 MPa or hydrostatically press it at about 48 to 200 kPa. Figure 6 summarizes the amounts of oxide starting materials and the final mineral phases that result.

This year, we have demonstrated that SYNROC has excellent immobilization properties and can be produced on a pilot-plant scale. The goal of our process-engineering research is to establish the feasibility of producing SYNROC on a larger scale under remote operation. Currently the process costs for defense wastes are higher for SYNROC than for borosilicate glass. However, since SYNROC can accept much higher waste loadings, the savings in repository costs would about balance its higher processing costs. SYNROC thus promises improved waste immobilization at costs comparable to those of current technology. Continued refinement of the SYNROC fabrication process will lead to further reductions in processing costs.

Studying Atmospheric CO_2 Concentration

During the past century, the global concentration of atmospheric carbon

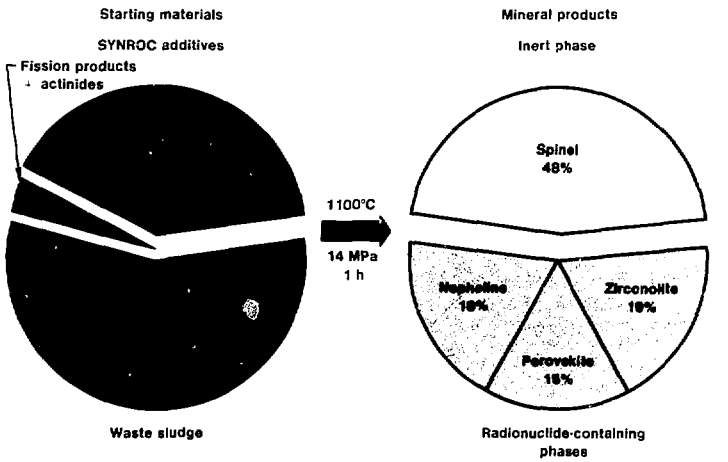

Fig. 6

Summary of the starting materials and mineral products of our SYNROC process. The emerald green areas represent the additives required to form the final SYNROC phases from the waste slurry (blue); note that this slurry contains a large proportion of nonradioactive material, primarily compounds of the transition metals iron, aluminum, and manganese. The final SYNROC phases can be divided into two groups, those that contain radionuclides (yellow green) and those that do not (gold).

dioxide has increased by 15 to 25%. Escalating emissions from fossil-fuel combustion could double concentrations by the second half of the next century. Such a trend could lead (through the so-called greenhouse effect) to a substantial warming of the earth's climate, with consequences for the biosphere that are uncertain but potentially disruptive. For example, changes in existing weather patterns could cause severe social, agricultural, and economic dislocations. Computer modeling by the Laboratory and other organizations indicates that doubling the atmospheric carbon dioxide would increase average global temperatures by about 2 to 3°C, with even greater warming in the polar regions.[9]

Continuous measurements from 1958 to the present, taken at the Mauna Loa Observatory in Hawaii, show that the atmospheric carbon dioxide concentration has increased from 315 to 340 ppmv in little less than a quarter century. Similar trends have been observed at other stations around the world. To determine the fraction of this trend resulting from fossil-fuel combustion and the fraction due to alterations of the biosphere (such as the destruction of tropical forests), it is necessary to understand the dynamics of the global carbon dioxide balance (the net concentration resulting from the action of sources and sinks). Critical to this balance is the magnitude and sign (plus or minus) of the net annual uptake of carbon dioxide by the oceans and the biosphere.

Accurate CO_2-exchange measurements in remote geographical areas can be difficult and costly. A method devised several years ago, called eddy correlation, uses sensors that can be carried by long-range aircraft to measure fluxes of atmospheric heat and water vapor. The application of this method to measuring carbon dioxide fluxes has awaited a sensor that is sufficiently fast and accurate. During the past several years, we developed such a sensor and demonstrated its ability to measure carbon dioxide fluxes over remote land and ocean surfaces.

Our high-resolution, fast-response sensor operates by measuring the differences in the absorption of infrared energy between wavelengths of 3.8 and 4.25 μm for various concentrations of carbon dioxide. We mount the sensor outside the fuselage of an aircraft so that the airstream flows through an open absorption cell in which it is exposed to an infrared beam (Fig. 7). The airstream is sampled 333 times a second, a rate equivalent to collecting an air sample every 30 cm along the aircraft's flight path. A long absorption path, necessary for high sensitivity, is obtained by reflecting the infrared beam across the open sample area several times with special mirrors. Accurate measurement of the carbon dioxide flux over some ocean areas requires a signal-to-noise ratio of more than 4000 to 1. The sensitivity and frequency response of our sensor meet this requirement, and it has a performance factor two orders of magnitude better than that of commercial sensors.

We recently confirmed the sensor's performance by remotely measuring, for the first time, carbon dioxide diffusion through the arctic icepack. Mounted on an aircraft belonging to the National Oceanic and Atmospheric Administration, the sensor collected nearly 10 h of detailed flux information over the ice and open water of the Bering Sea and over the ice of the Arctic Ocean. We have also tested it in a tower-mounted design to measure carbon dioxide fluxes over crops and vegetated areas. The sensor's widespread use should provide a wealth of otherwise unattainable information on the dynamics of the global carbon dioxide balance.

Liquefied Natural Gas Safety

The growing volume of liquefied gaseous fuels transported and stored around the world increases the possibility of very large spills from storage-tank or ship accidents, with potentially disastrous effects. If such a spill occurred in or near an inhabited area, the almost inevitable ignition could cause

widespread destruction. Our Liquefied Gaseous Fuels Spill Effects Program was established by the DOE to develop and validate methods of predicting the consequences of such spills so that they can be better controlled. These consequences include pool spread, vaporization, dispersion, ignition, combustion, explosion, and damage effects.

We are conducting experiments to obtain data on the atmospheric dispersion characteristics of denser-than-air gases and the combustion physics of large vapor clouds.[10] These data are used to develop an ensemble of computer models to predict spill behavior under conditions that cannot be experimentally replicated. In 1980 and again

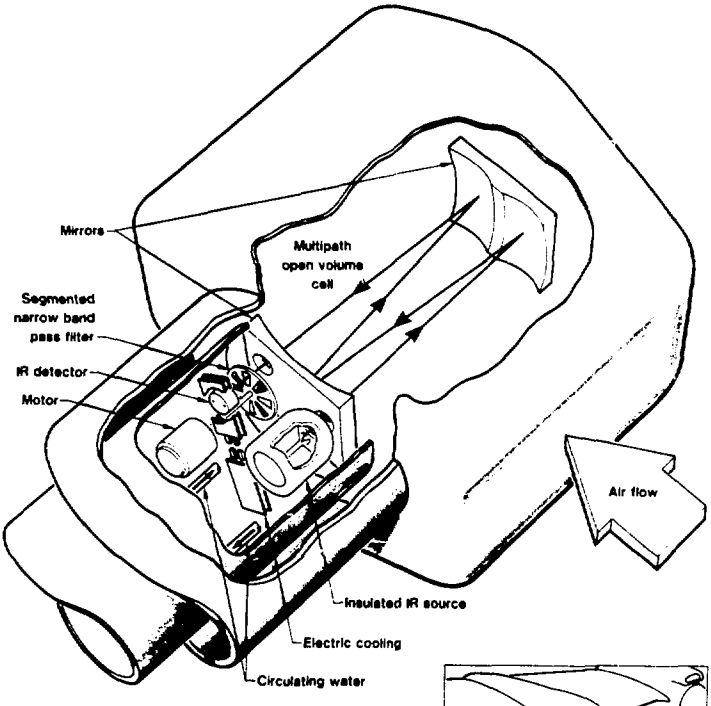

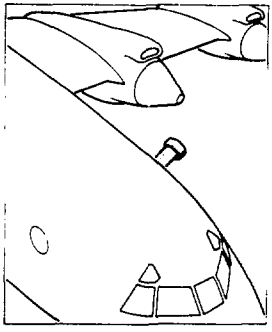

Fig. 7

Mounted on an aircraft (inset), the carbon dioxide flux-measuring sensor correlates the concentration of carbon dioxide, temperature, pressure, and humidity with eddies moving upward and downward over a land or sea surface. The undisturbed airstream moves through the sensor's open, multipath absorption cell. Carbon dioxide concentration is measured by comparing unabsorbed infrared wavelengths with those attenuated by carbon dioxide.

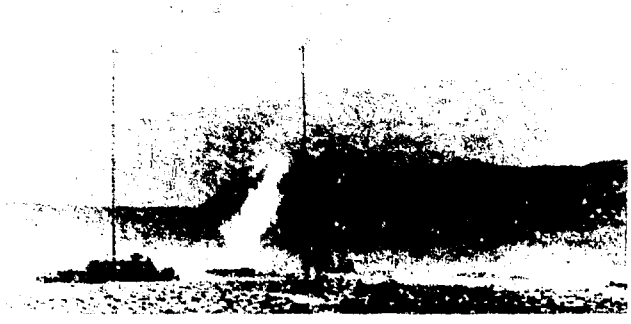

Fig. 8

Combustion of the vapor cloud formed when 40 m^3 of liquefied natural gas was spilled into a man-made pond. The experiment, conducted at China Lake, California, provided a variety of data on spill behavior and combustion physics. Data were recorded by a large array of sensors. Note the heat-distorted image of the hills in the background.

in 1981, we conducted a series of tests at the U.S. Naval Weapons Center at China Lake, California, in which 40 m^3 of liquefied natural gas (LNG) per test were spilled and ignited. The spills formed cold, heavy vapor clouds that were flammable as much as 400 m downwind (Fig. 8).

To gather data on the formation, dispersion, and combusion of the gas cloud, we deployed a variety of instruments in an extensive array upwind and downwind of the spill point. Anemometers at 26 stations mapped the wind field. The gas cloud was tracked and measured at 31 stations with a variety of gas sensors; some measured methane and higher hydrocarbons separately and others sensed total hydrocarbons.[11] Data on the burning gas were obtained with thermocouples, burn-velocity and heat-flux sensors, and pressure transducers. Cameras and infrared imagers made remote measurements. All experimental stations were battery powered and microprocessor controlled. We communicated with the stations by computer-controlled radio telemetry, switching on their power and receiving their data by remote command. The trailer that housed the central computers and the data-recording equipment was located about 1200 m from the experimental area.

Our results indicate that large, dense clouds of LNG disperse in the atmosphere very differently from neutral-density clouds and may produce a more hazardous situation than expected on the basis of small-scale tests.

Because the constituents of LNG boil at different temperatures, large spills also produce clouds containing regions enriched in heavier hydrocarbons. These regions are more detonable than the rest of the cloud. In some tests, rapid-phase-transition (RPT) explosions unexpectedly occurred when a quantity of LNG suddenly vaporized, expanding in volume over 200 times, nearly instantaneously. As many as 20 RPT explosions took place during one 40-m^3 LNG spill. The largest had a measured peak pressure equivalent to 6 kg of TNT. Our experiments demonstrated that RPT explosions may play an important role in determining the outcome of an accident.

In some tests, the gas cloud was ignited at the end of the spill with flares or a flame-jet igniter. The ignition point was about 90 m from the spill point. The flame front moved rapidly downwind and upwind from the ignition point, enveloping an area about 100 m wide and 300 m long. We observed flame speeds between 12 and 19 m/s. The vapor burn tests revealed larger fires and faster flames than had been observed previously.

A comparison of model predictions with dispersion data from the tests was encouraging. In the next step, we will introduce terrain effects into the models. These experiments were an important step toward understanding the dispersion behavior and combustion physics of very large spills of liquefied gaseous fuels. Further experimental data from spills of 100 to 200 m^3 will be crucial to answering the many remaining questions about this hazard.

Biomedical Sciences

The effects of cell damage caused by environmental pollutants is a field of continuing concern. We are conducting a variety of biomedical studies into the mechanisms of cellular change and the identification of potentially damaging agents (e.g., radiation and chemicals). These include studies of morphological changes in sperm, of processes of gene damage and repair, and of chromosome changes caused by damaged DNA. We

are also developing techniques for quickly screening potential mutagens.

Sperm Studies

Spermatogenesis, the production of sperm, is essential to reproduction in many biological species. Because sperm are exquisitely sensitive to external influences, they can serve as an important dosimeter of biological changes caused by chemical or radiological agents. Advances in sperm assay (the process of measuring and interpreting these changes) require, among other things, a better understanding of sperm characteristics. At LLNL, we are developing new techniques of sperm assay based on our own discoveries and the work of others and applying them to a variety of mammals, including man. During the past year, we have made important progress in measuring sperm morphology, in understanding the mechanism of genetic packaging in sperm, in identifying chromosomal changes, and in developing techniques that could lead to control of the sex ratio in reproduction.

Assaying sperm morphology. For several years, LLNL has pioneered the microscopic assay of sperm shape, emphasizing its application to human studies. During spermatogenesis, sperm are transformed from spherical cells into bodies with leaf-shaped heads and long, undulating tails. This process, which is controlled by many genes, is highly sensitive to genetic and physiological conditions that can produce abnormal cell shapes. Our population studies have shown that in both mice and men, the fraction of abnormal sperm found in individuals can respond dramatically to radiation or to chemical mutagens; there also is evidence that such abnormalities of sperm production in x-irradiated mice may be permanent and heritable.

Detecting abnormal sperm shapes by visual examination is a slow and somewhat subjective process. We are developing automated, quantitative methods of shape detection that are both faster and more sensitive than conventional techniques. In one approach, called slit-scan flow cytometry (SSFCM), sperm stained with a fluorescent dye flow single file through a very narrow (1- to 2-μm-wide) laser beam. Each sperm produces a fluorescence profile that is recorded and analyzed by a computer. Figure 9 shows typical SSFCM profiles obtained from four different kinds of mammalian sperm. The shape of a profile, which is species-specific in mammals, is different in abnormal sperm. We have used this

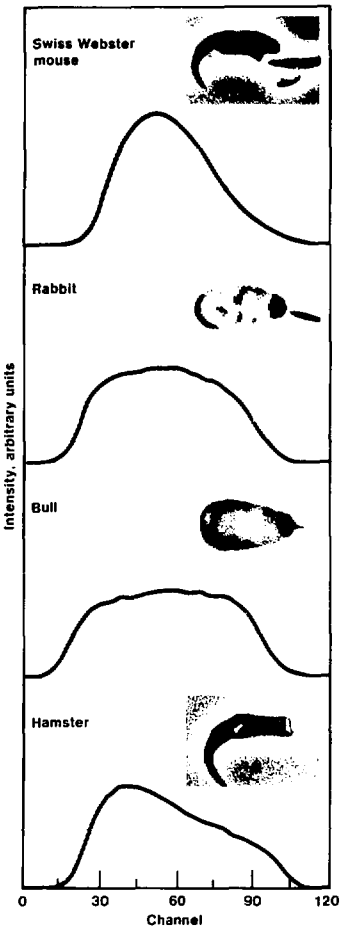

Fig. 9

Four mammalian sperm profiles obtained by automated screening, using SSFCM of many sperm cells of each species. Sperm were stained with a fluorescent dye and passed, single-file, through a very narrow laser beam. The fluorescence profiles produced were recorded and analyzed by computer. The insets are photomicrographs of corresponding sperm cells (the scale is about the same in all photographs).

technique to detect radiation-induced changes in mouse sperm, with results equal in sensitivity to those of visual assessment. We have found that SSFCM shape measurements provide high-speed analysis (currently about 100 cell/s) with a statistical precision greater than that obtainable with any other method of comparable speed.

In another approach, we use a scanning microscope and computer to assess sperm morphology. The image of each sperm is digitized by the microscope at a resolution of 16 pixels (picture elements) per square micrometre. The computer locates the outline of the sperm head and extracts from it a variety of shape parameters. We find that the heads of mouse sperm exposed to increasingly larger doses of x rays become smaller and more circular.

Genetic packaging in sperm. The ability of mammalian sperm to carry vast amounts of genetic information in a nucleus apparently large enough to contain only one fourth of the genetic material has long been a puzzle. We have found that the nuclei of mouse sperm, for example, contain 3.3 pg of deoxyribonucleic acid (DNA, the material of the genes, which in turn make up the chromosomes). Known mechanisms of packing this amount of DNA would require twice the available volume of the sperm nucleus. In addition, sperm nuclei contain 3 pg of protamine, a protein unique to these cells. Together with the DNA, this amount of protamine would increase the space needed by at least four times what is available.

Our biochemical studies and scanning-microscope measurements have provided the first explanation of this phenomenon. The key to understanding the tight packing lies in protamine. Whereas DNA carries a negative electrical charge, protamine has a strong positive charge. This enables protamine to bind to the minor groove in DNA's double helix, electrically neutralizing it. Chromosomes formed of this neutralized DNA can be so tightly packed that they fit the restricted volume available. In a sperm nucleus, thousands of these DNA-protamine complexes join together. In doing so, they both effectively shut off the sperm's genetic machinery and simultaneously protect it from potentially harmful substances. Except for certain regions of the human sperm, which appear to be packed differently, the sperm of most species seem to be organized in this way.

Sexing sperm. The sex of most mammals is determined by a specific chromosome in the fertilizing sperm, a Y chromosome producing a male offspring and an X chromosome a female. As the X chromosome is larger than the Y, half of an individual's sperm should be correspondingly richer in DNA. A means of distinguishing and separating sperm cells according to DNA content would thus raise the possibility of controlling or influencing the sex of the fertilized egg.

We have developed a hydrodynamic method of orienting flat mammalian sperm in flow instruments to permit optical measurements of the DNA content of individual cells. We have resolved the sperm populations bearing X and Y chromosomes in several mammals, including bulls, boars, rams, rabbits, mice, and voles. In addition, we have identified the relative proportion of X and Y sperm in samples of cryopreserved bull semen.

This method should find immediate application in monitoring and accelerating the further development of X-Y sperm-separation techniques. In the longer run, the prospect of controlling the sex ratio at birth by fertilizing eggs with selected sperm has considerable implications for stock breeding and animal husbandry. The ability, for example, to optimize proportions of males and females with sex-specific traits such as milk and egg production or rate of weight gain would have an immediate payoff in raising the efficiency of food producers.

Chromosome Damage and Mutations

Physical and chemical substances in the environment can interact with DNA

in the body's cells in various ways to produce damage that is biologically deleterious. Persons who are genetically deficient in mechanisms that correct DNA damage may be hypersensitive to cancers or heritable disorders. In the disease xeroderma pigmentosum, for example, the victim develops skin cancer presumably because his cells are unable to repair the damage to DNA caused by ultraviolet light. It is thus important to understand the nature of the initial damage to DNA and the processes by which the damage is either repaired or expressed as a heritable mutation, a chromosomal alteration, or the death of the cell. During the past year, we have made substantial progress toward understanding cellular repair processes and have applied some new cytogenetic methods to detect and quantify damage in exposed persons.

Repair-deficient hamster cells. As DNA repair processes are believed to be similar in most mammals, we used cells from the Chinese hamster, which can be easily grown and manipulated in the laboratory. By exposing the cells to ultraviolet light, we isolated several mutants that, because of defects in their processes that normally repair DNA damage, were hypersensitive to the cell-killing effect of this agent. More specifically, the cells appeared to lack one step in the process that removes the ultraviolet-caused lesion from the DNA. In this respect, the defect in hamster cells is analogous to the deficiency causing xeroderma pigmentosum in humans.

Hamster cells sensitive to the killing effects of ultraviolet light are also hypersensitive to mutations and to sister chromatid exchange (SCE), a type of chromosome damage induced by a variety of chemicals. In SCE, which can be observed through a light microscope (Fig. 10), DNA is exchanged between the two halves (chromatids) of a chromosome. We have found that ultraviolet-induced lesions that cause SCEs persist in repair-deficient hamster cells but not in cells that can repair damage. Our results suggest that unrepaired lesions in DNA may be responsible for the chemically induced increase in both the frequency of mutation production and the frequency of SCE.

Fig. 10

Chromosomes from a human lymphocyte, stained to demonstrate sister chromatid exchange (SCE). In a chromosome without an SCE, one arm (chromatid) stains dark and the other light. In a chromosome in which SCE has occurred, dark and light regions in the same arm reveal that portions of the chromatids have been interchanged (arrows).

We are using these mutant hamster cells to search for a human gene involved in the repair of DNA damage. To do this, we first fuse hamster cells with human cells to form a hybrid cell containing chromosomes from both species. Human chromosomes in the hybrid are preferentially and randomly lost when the cell divides. We then expose the hybrid cells to continued chemical stress; those that are repair-deficient die. The hybrids that survive contain one or more human chromosomes. It appears, then, that certain human chromosomes confer resistance on the hamster cells by supplying a gene

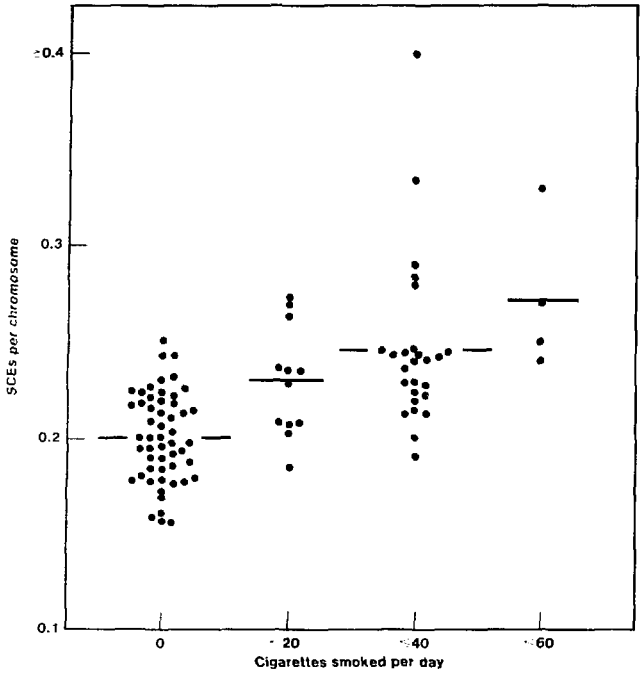

Fig. 11

Frequency of SCE measured in lymphocytes of cigarette smokers as a function of the number of cigarettes smoked per day. Each data point represents a single subject. Significant increases in SCE frequency were observed in smokers as a group, though not in every subject; some nonsmokers also showed a high SCE frequency.

able to repair the chemical damage. We are analyzing the surviving hybrids to identify the human chromosome carrying this gene.

Sister chromatid exchange in humans. As noted above, sister chromatid exchange is an interchange between the two double helices of a replicated chromosome. At the molecular level, this event indicates that the DNA was broken and rejoined. It is not known with certainty, however, whether the rejoining process is accurate, leaving the DNA sequence unchanged, or whether it might introduce a mutation.

We examined the ability of different substances to induce both SCE and mutations in Chinese hamster cells. Our results showed a linear relation between induced SCE and induced gene mutation. If SCE reflects mutagenic insult, both industrial hygiene and epidemiology would be advanced by measurements of the SCE frequency in circulating blood lymphocytes of persons occupationally or otherwise exposed to mutagenic agents.

We have measured SCE frequency in cigarette smokers, a group that is known to be at increased risk for developing lung cancer. Our results show that the frequency of SCE in blood lymphocytes of LLNL smokers is higher than normal and depends on the number of cigarettes smoked per day (Fig. 11). We also found considerable variation among individuals, some smokers showing no increase. Other studies we have conducted indicate that the individual differences reflect both genetic factors and exposure to additional agents such as medications or occupational substances. Preliminary data from a follow-up study indicate that increased SCE frequency persists for at least six months in some subjects who stop smoking. Our studies have established the utility of SCE in detecting exposure to human mutagens. Further research is needed to explore the clinical significance of these findings. ■

Key Words: aluminum-air power cell; carbon dioxide—balance, sensor; coal gasification; controlled retraction of the injection point (CRIP); electric vehicle; genetic packing; liquefied natural gas; Liquefied Gaseous Fuels Spill Effects Program; Local Control and Instrumentation System (LCIS); magnetic fusion energy (MFE); Mirror Fusion Test Facility (MFTF); MFTF-B; mutagen; protamine; radioactive waste storage; sister chromatid exchange (SCE); slit-scan flow cytometry (SSFCM); sperm—morphlogy, sexing; Supervisory Control and Diagnostic System (SCDS); SYNROC; Tandem Mirror Experiment (TMX); xeroderma pigmentosum.

Notes and References

1. *TMX experimental results were reported in Energy and Technology Review*, June 1981 (UCRL-52000-81-6), p. 1.
2. The scope of the MFTF project was changed in 1980 as plans were made to convert it to a very large tandem mirror experiment (MFTF-B). For a discussion of MFTF-B, see the July 1980 *Energy and Technology Review* (UCRL-52000-80-7), p. 1.
3. The principles of the aluminum-air battery were discussed in *Energy and Technology*

Review, November 1980 (UCRL-52000-80-11), p. 1.

4. For a discussion of an earlier LLNL experiment in coal gasification, see *Energy and Technology Review*, May 1980 (UCRL-52000-80-5), p. 17.
5. R. W. Hill and M. J. Shannon, *The Controlled Retracting Injection Point (CRIP) System: A Modified Steam Method for In Situ Coal Gasification*, Lawrence Livermore National Laboratory, Rept. UCRL-85852 (1981).
6. The Laboratory's SYNROC process was described in detail in *Energy and Technology Review*, December 1981 (UCRL-52000-81-12), p. 13.
7. A. E. Ringwood, *Safe Disposal of High-Level Nuclear Reactor Wastes: A New Strategy*, Australian National University Press, Canberra, Australia, and Noroalk, Conn., USA, 1978; and A.E. Ringwood, S.E. Kesson, N.G. Ware, W.O. Hibberson, and A. Major, "The SYNROC Process: A Geochemical Approach to Nuclear Waste Immobilization," *Geochem. J.* **13**, 141 (1979).
8. J. Campbell, C. Hoenig, E. Bazan, E. Ryerson, M. Guinan, R. Van and R. Rozsa, *Properties of SYNROC-D Nuclear Waste Form: A State of the Art Review*, Lawrence Livermore National Laboratory, Rept. UCRL-53240 (1982).
9. The problem of identifying global changes in atmospheric carbon dioxide was reviewed in M. C. MacCracken and H. Moses, *The Past Detection of Carbon Dioxide Effects Workshop Summary*, Lawrence Livermore National Laboratory, Rept. UCRL-87302 (1982).
10. Earlier Laboratory experiments with LNG spills were reported in *Energy and Technology Review*, October 1980 (UCRL-52000-80-10), p. 27.
11. The Laboratory's portable hydrocarbon sensor was described in *Energy and Technology Review*, September 1980 (UCRL-52000-80-9), p. 36.

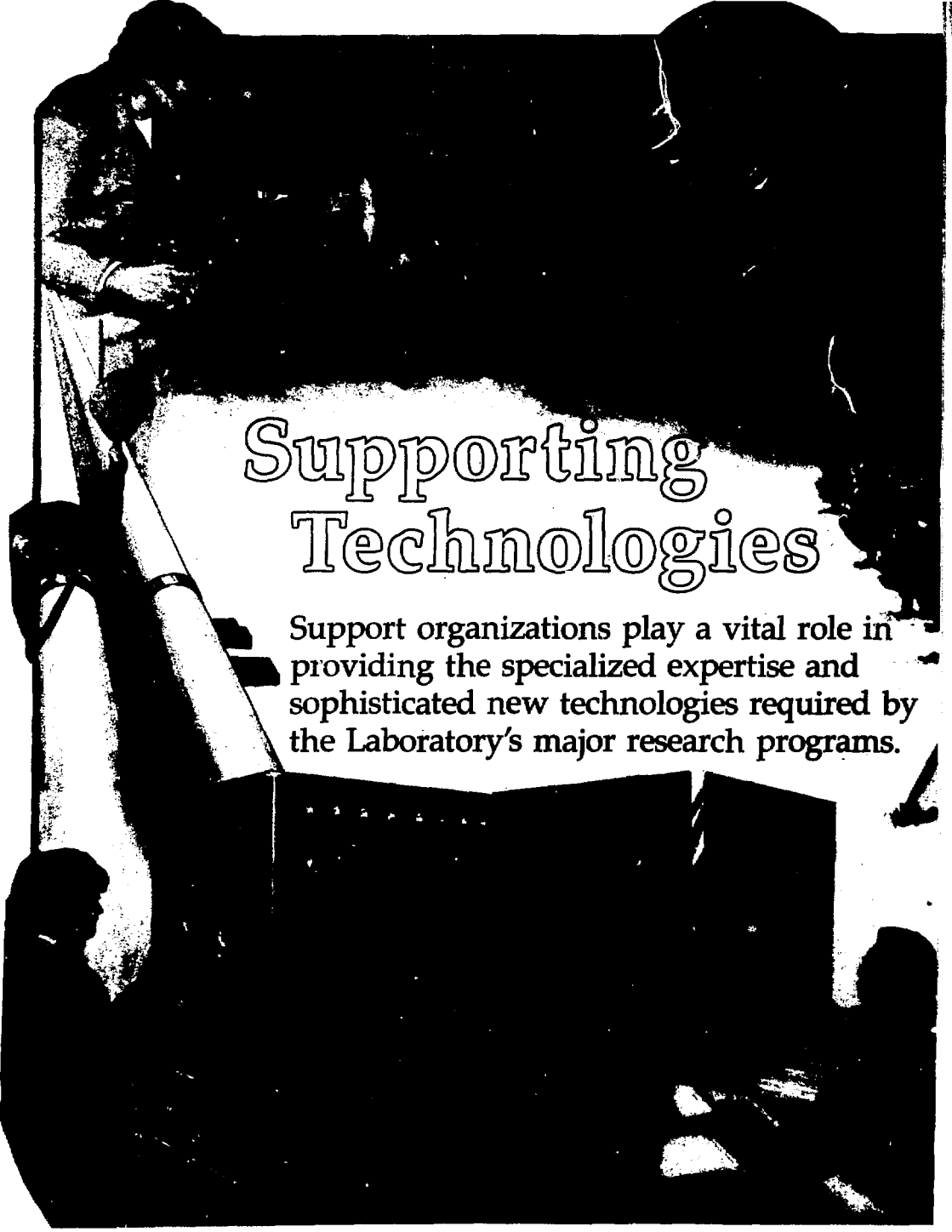

Supporting Technologies

Support organizations play a vital role in providing the specialized expertise and sophisticated new technologies required by the Laboratory's major research programs.

The Laboratory's major programs in weapons, magnetic fusion energy, laser fusion, laser isotope separation, biomedicine, and environmental science generate constantly evolving needs for new research tools and techniques. Support departments operating through LLNL's matrix structure provide a pool of specialized professionals who can provide prompt and flexible assistance to these programs over a broad and diverse range of disciplines.

In our matrix structure, individuals can work under the immediate supervision of a multidisciplinary program such as magnetic fusion energy while retaining membership in a specialized support department such as physics, chemistry, engineering, or computations. This structure encourages the pooling of expertise in special disciplines and technologies as well as active interactions among support groups to solve technical problems as they arise in programmatic research.

This fruitful process often leads to innovations that have applications in the larger technical community as well as to specific problems at the Laboratory. For example, new instruments incorporating fiber-optics technology that we developed for remotely monitoring the physical and chemical properties of highly radioactive materials may be useful to industries working with hazardous processes of various kinds. A new technique for increasing the accuracy of measurements made on precisely machined, contoured surfaces has equally broad applicability.

In addition to illustrating the success of our matrix approach, the sampling of support projects reviewed in this article represents important contributions to a variety of fields. They include remote analysis with optical fibers, a high-speed camera, an oil-showered precision measurement machine, a small diamond turning lathe, new instruments for probing hot, very dense plasmas, precision machining of large crystals for new lasers, a satellite link for the nation's magnetic fusion energy program, a cooperative effort with Japan to expand our magnetic fusion materials facility, and a study of breakdown mechanisms in semiconductors exposed to electromagnetic pulses.

Remote Analysis with Optical Fibers

Many industrial processes or other phenomena of interest cannot be measured with conventional instruments because they are too hot, too cold, highly radioactive, or otherwise inaccessible to direct observation. Nuclear wastes stored in underground repositories, for example, will require monitoring *in situ*. A new technology that uses long-distance fiber optics to transmit laser-excited fluorescence now makes it possible to remotely monitor such phenomena via optical fiber cables at distances up to a kilometre.

We have put together a basic system consisting of a laser light source, a Raman-fluorescence scattering spectrometer, and an optical fiber linked to a measuring device at the other end. Laser-generated light passes through an aperture and is focused on the end of the optical fiber by a geometric beam splitter (Fig. 1). The light passes through the fiber, interacts with the sample to be measured, and returns (now incoherent), to be reflected by a mirror into the computerized spectrometer for analysis. Measurements are made either at the bare fiber terminus or by an optrode, a complex measuring device coupled to the fiber and containing sensitive fluorescing layers that interact with the sample.

This optical fiber system for remote measurements should find wide application wherever phenomena of interest are too hazardous for direct observation.

A High-Speed Image-Converter Camera System

Multiframe cameras, both mechanical and electronic, are widely used in science and engineering. At the Laboratory, we use these cameras to record fine physical details of very rapid events such as the surface behavior of explosively driven materials. We have found that in certain applications,

commercially available multiframe cameras have several deficiencies: an image size that restricts spatial resolution, an inflexible framing rate, and magnification that is limited to one choice per experiment.

We have developed a new camera design, based on image conversion, that remedies these deficiencies and meets our present and projected needs for high-resolution, stop-action photography of high-velocity objects. At our request, a U.S. manufacturer developed a large image-converter (IC) tube (essentially a high-speed electronic shutter) that met our specifications for size and performance. We incorporated this tube in a camera designed to:

- Record rapidly moving objects (velocities up to several millimetres per microsecond) without blurring at exposures of 10 to 50 ns.
- Provide a dynamic spatial resolution at the film plane of 10 line-pairs/mm.
- View the subject along four optical paths providing four different magnifications.
- Expose eight frames, independently assigned within a time window of tens of microseconds.
- Provide a photographic format 75 mm in diameter.
- Operate at a high ambient-light level.

The camera is quite simple in principle, consisting of four viewing paths, each comprising an optical system, two gated IC tubes, and two frames of recording film. Light from the subject passes through an f/5 objective, a multielement relay lens, a beam splitter that sends an image to both IC tubes, and a field flattener at each tube that restores the planarity of the image. Each viewing path provides individual magnification to record simultaneously different details of the subject. A high-quality image is present at the 75-mm proximity-focused IC tube any time the mechanical shutter is open. The image is transmitted to the recording film in response to a preassigned 10-kV "gate" pulse produced by novel electronic circuitry. (In addition to rapid gating, the IC tube provides a modest light gain.) The temporal width of the pulse can be selected for each frame independently within a range of 10 to 50 ns; pulse width is easily adjusted at the control panel. The positions of the gate pulses in time are virtually unlimited.

The IC camera was originally designed to incorporate a multipulse laser illumination system that spectrally excludes background light. However, we have successfully used it without a laser to photograph self-luminous objects such as expoding bridgewires.

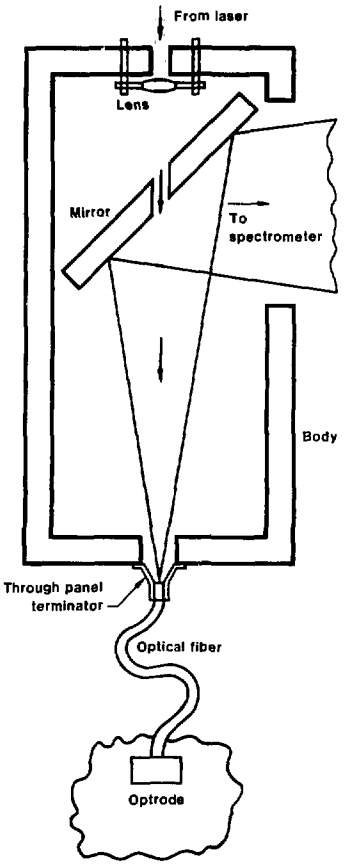

Fig. 1

Remote-analysis fiber-optics system. Light from a laser source passes through an aperture and is focused on the end of the optical fiber by a geometric beam splitter. The light passes through the fiber, interacts with the sample to be measured, and returns (now incoherent), to be reflected by a mirror into a computerized Raman-fluorescence scattering spectrometer for analysis. Measurements are made at the sample by an optrode or by the bare fiber terminus, which can be coated to fluoresce in response to certain substances.

Fig. 2

An exploding bridgewire photographed with our high-speed, multiframe IC camera. (a) A front-lighted photograph of the bridgewire (the narrow strip in the center) before detonation. The current flows upward in the photograph. Bridgewire dimensions are 254 μm wide by 635 μm long; the magnification is 18:1. (b) Emission from a bridgewire during normal detonation. The exposure time is 10 ns. Hot spots are visible at the corners where the bridgewire meets the attaching conductor. Self-luminance spreads laterally to about 1.8 times the width of the bridgewire. (c) An abnormal explosion in which self-luminance quickly moves laterally to seven times the width of the conductor, indicating the spread of shock energy over an area larger than normal. Thermal cycling produces an air gap between the bridgewire and the surface of the explosive, thwarting predictable detonation.

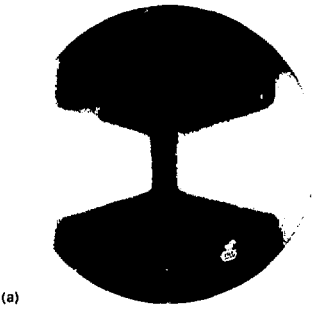

(a)

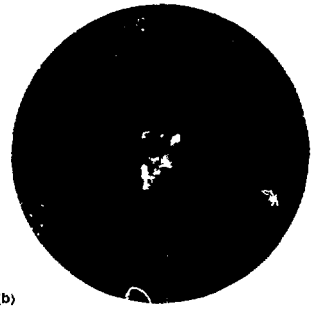

(b)

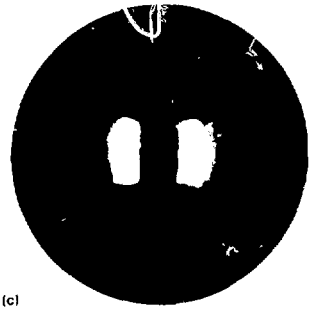

(c)

Exploding bridgewires are widely used to detonate high explosives, an application that demands reliable performance. In certain temperature-cycling sequences and test geometries, however, an exploding bridgewire may fail to perform normally. In such cases, the temperature cycling has caused the explosive to contract, producing an air gap between itself and the bridgewire detonator. This gap prevents the energy of the detonator from coupling efficiently to the explosive.

We have applied the IC camera to record visible emission from an exploding bridgewire during normal and abnormal (failed) operation (Fig. 2). The exposure time was 10 ns. During a normal explosion, self-luminance covers the area of the conductor laterally to about 1.8 times the width of the bridgewire. Hot spots are visible at the corners where the bridgewire meets the conductor that attaches to the explosive. In an abnormal explosion, however, self-luminance quickly moves laterally to seven times the width of the conductor, indicating the spread of shock energy over an area larger than normal. Multiple-frame records suggest that the velocity of the luminous front is a few millimetres per microsecond. This recording process reveals that the air gap, caused by thermal cycling, thwarts predictable detonation.

The IC camera's excellent image quality, rapid gating, and versatile framing time have dramatically improved our ability to record high-velocity phenomena.

An Oil-Showered Precison Measurement Machine

The Laboratory has pioneered many diamond-turning and precison-machining technologies that are now universally used. Our own two large diamond-turning machines are designed to produce contoured surfaces with great precision (± 0.25 μm for one and ± 0.05 μm for the other). For some years, in fact, the precision of these machines has exceeded the accuracy of available measuring devices.

Last year, we rectified this situation by completing modification of a contour measurement machine that is ten times more accurate than the original. For the first time in several years, we now have an inspection machine more accurate than the parts it measures. We believe this to be the world's first liquid-showered, general-purpose

measuring machine. It has been in regular use at LLNL for the past year.

The principal problem in achieving accurate measurements is thermal drift caused by changes in the ambient temperature. Neither air-temperature nor air-velocity controls are adequate to check this drift. Our modification uses an oil shower to control temperature and a laser interferometer to make measurements. The crucial innovation, however, is the oil shower, as the interferometer alone would be superfluous without effective temperature control. We believe the machine to be unique in this respect.

During a measurement, all surfaces of the machine, including the part being measured, are showered with temperature-controlled oil, forming a flowing layer that isolates the system from the room environment (Fig. 3). The temperature of the oil is maintained at a nominal 20°C; maximum variation is 0.006°C averaged over 30 s. A simple on-off system controls the supply of chilled water to a shell-and-tube heat exchanger. The entire volume of oil is recirculated through the loop once a minute at a rate of 150 l/min.

The oil-shower technique reduces thermal drift to 0.10 μm measured over a period of 8 h. In contrast, thermal drift measured in the same room in the absence of an oil shower was 20 μm. This accuracy enables the machine to make repeatable measurements within 0.10 μm.

The presence of flowing oil is manageable, though the machine is not as comfortable to operate as a dry machine. The operator must work with his hands in oil, and some daily housekeeping is needed to keep the work area safe and clean. The simplicity and effectiveness of this temperature-control technique, however, more than compensate for these inconveniences.

This oil-shower technique of controlling thermal drift has also been applied at the Laboratory to the machining of large single crystals to the extremely close tolerances required by the Nova and Novette lasers (see the section beginning on p. 46).

Baby Optics Diamond Turning Machine

In 1981, we were faced with an urgent requirement for a high-precision diamond lathe able to machine a variety of contoured parts less than about 10 cm in diameter to tolerances comparable to those of our large diamond turning machines. Although several commercially available machines met these specifications, time constraints led us to design our own machine and to assemble it in two weeks from parts on hand.

Our design criteria were:

- To minimize sources of nonrepeatable error, such as those arising from thermal effects.

Fig. 3

The Laboratory's oil-showered precision measurement machine. Both the machine and the part being measured are maintained at a constant temperature by a temperature-controlled oil shower that isolates the system from its thermal environment.

Fig. 4

LLNL's baby optics diamond turning machine, designed and assembled in two weeks from parts on hand. The success of this effort demonstrates that the design of such high-precision machine tools is a mature technology.

- To minimize sources of random spindle motion, such as vibrations from the drive motor.

To solve these problems within the time available, we constructed a machine (Fig. 4) smaller than our existing diamond lathes. The baby machine has crossed roller slides with 15 cm of travel. The straightness of travel of the x slide is 1.1 μm over 10 cm, and of the z slide 1 μm over 10 cm. The base of the machine is a granite surface plate lapped to a flatness of 0.5 μm over the area occupied by the slides. Three rubber pads support the base to isolate the system from vibration.

The air-bearing spindle has an average axial and radial motion of less than 25 nm. It is driven by a dc servo-drive motor, which with our electronics package can deliver up to 11 Nm of torque at any speed from 50 to 2000 rpm. To control spindle temperature, we circulate about 20 l/min of temperature-controlled water through the spindle motor housing. Ambient air temperature is controlled to about 20 ± 0.1°C. In addition, we reduced thermal effects by minimizing critical dimensions such as the distance between the x-axis interferometer and the tool post.

We used a computer numerical controller configured to interface with the position-feedback system. The feedback system consists of a laser interferometer and an interface package operating at a resolution of 25 nm.

Had more time been available, we might have implemented a more conventional design, including a larger machine with air-bearing slides, improved leadscrews, a more elaborate temperature-control system, and self-leveling pneumatic vibration isolators. However, our success with the off-the-shelf approach demonstrates that the design of high-precision diamond turning machines is a mature technology. Given adequate human resources, machines comparable in accuracy to existing machines can be assembled from commercial components. In this instance, the size of our baby machine worked together with our design criteria to produce a system that is relatively immune to both vibration sources and temperature variations.

Machining KDP Crystals

We have used diamond turning tools to machine large single crystals of potassium dihydrogen phosphate (KDP) to extraordinarily close tolerances for optical components of the Nova and Novette lasers. These crystals convert infrared laser light (wavelength 1.053 μm) to its green and blue harmonics (0.527 and 0.351 μm, respectively). Light at these wavelengths significantly improves laser-driven implosion.[1] For a KDP crystal to generate these harmonics most efficiently, its face must be machined exactly perpendicular to the optical axis.

In support of the Laboratory's inertial-confinement fusion program, the Materials Fabrication Division (MFD) has successfully machined 50 KDP crystals, with another 15 in process. Because single crystals of KDP are

Fig. 5

KDP crystal machined to extraordinarily close tolerances. The top surface has an area of 5 cm^2. Crystals like this will be used with the Nova and Novette lasers for inertial-confinement fusion research. We had to solve several problems to machine the crystal, including a high coefficient of thermal expansion, brittleness, low tensile strength, and change of optical axis with temperature.

not available in a large enough size to match the 74-cm-diam laser beam of Nova and Novette, the aperture will be made up of KDP tiles positioned in an array. We machine three sizes of KDP tiles. The smallest, used for the feasibility demonstration, is 5 cm^2 (Fig. 5). The largest, 27 cm^2, will be used for Nova. The medium size, 15 cm^2, will be used for the first arm of Novette because of material availability: it takes nine months to grow a KDP crystal from solution.

KDP presented a number of machining problems. It is sensitive to moisture. It is anisotropic, with a large coefficient of thermal expansion, 44 ppm/°C, or twice that of aluminum. The optical axis (the direction of maximum conversion to harmonics) changes with temperature. The crystal is also brittle and has a very low tensile strength. We had to solve these machining problems and achieve the following tolerances: flatness, 2 μm; thickness, ± 1 μm from nominal; thickness waviness, 0.25 μm in 2.5 mm; optical axis perpendicular to face, ± 29 μrad; surface finish, 0.025 μm Ra (arithmetic average); and edge geometry, ± 10 μm. We were able to hold these tolerances to within half of their allowable values, with a negligible scrap rate, while working two and a half shifts (20 h) a day to maintain our production schedule.

Several techniques were used to achieve these results. First, KDP can be diamond-turned without tool wear by using a 45-deg negative rake angle (a technique first suggested in MFD's Glass Machining Research Program). The crystals were turned with one of LLNL's ultraprecise diamond turning machines, which has a repeatability of 0.025 μm. We reduced the temperature sensitivity of the KDP crystals to a minor factor by controlling the temperature of the machines at 20 $\pm$ 0.05°C with a 150-l/min oil shower (see the article on p. 44 of this issue). Since the oil had a negligible water content, this technique also eliminated the moisture sensitivity problem. Finally, dedicated skill and careful handling enabled us to meet the extraordinary tolerances required in the KDP crystals.

Fig. 6

Time sequence of pinhole photographs showing neon x rays produced in a plasma with the ZAPP device. The exposure times and intervals between photographs were 2 ns. The time direction is to the right; the last frame is time-integrated.

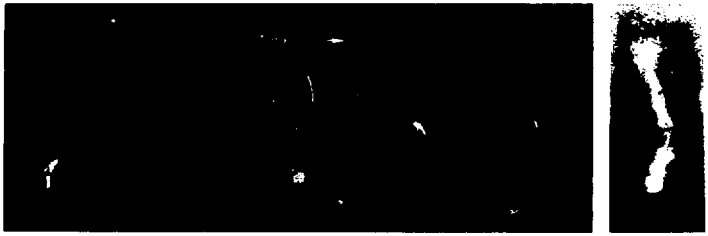

ZAPP Upgraded

Our z-pinch facility (ZAPP, for Z-pinch Atomic Physics Project)[2] has been upgraded by the addition of several new diagnostic instruments. ZAPP was designed to study in detail the radiation emitted by very hot, dense plasmas. A z pinch (z being the axial direction) is a cylindrical implosion caused by the self-induced magnetic field of a heavy current flowing through a plasma.

The ZAPP device consists of a large capacitor bank (52 kJ maximum) for storing electrical charge, fast electrical switches, and a vacuum chamber into which we can inject a hollow cylindrical puff of gas through an annular slit centered in the face of a flat electrode. The gas crosses a gap of about 1 cm to a ring-shaped electrode, which is pulsed to a high voltage before the gas has time to fill the center of the puff. A heavy current from the capacitor bank ionizes the gas and then implodes it by interaction with its self-generated magnetic field. Since the initial plasma is hollow, the final forces opposing the implosion are reduced, and the plasma can reach higher densities and temperatures than those in previous z-pinch devices.

At the ZAPP facility, we can consistently produce argon plasmas with electron temperatures of 1 keV and a density of 10^{22} electron/cm^3, a regime that until recently has been very difficult to achieve in the laboratory. These temperature and density conditions significantly affect the populations and lifetimes of the electronic states in the plasma. Our experimental studies of these plasmas have possible applications in fields as diverse as astrophysics and laser fusion.

We use a variety of techniques to obtain information on plasma conditions and atomic radiation in the ZAPP device, including crystal, normal-, and grazing-incidence spectrometry, pinhole and Schlieren photography, interferometry, and Thomson scattering.

Last year, we built and added to ZAPP three diagnostic instruments that incorporate a microchannel plate (MCP) camera. In the MCP, incident photons produce an electron cascade across a voltage in a narrow channel. The amplification thus achieved makes it a highly sensitive photon detector. The new diagnostic instruments are a crystal x-ray spectrometer, a pinhole camera, and a grazing-incidence spectrometer. Together, they give us the ability to analyze photon emission with high spatial, spectral, and temporal resolution in the ultraviolet and x-ray regions of the electromagnetic spectrum.

We independently tested the MCP camera used in these instruments to determine its sensitivity and limits of spatial and temporal resolution. So sensitive are MCPs that they have been shown to be capable of counting individual photons. Under these conditions, sensitivity is limited only by the MCP's quantum efficiency. This represents an increase of two to three orders of magnitude over ordinary photographic film. We tested the camera's spatial resolution using a grating spectrometer and a cold cathode line source, achieving a resolution of less than 50 μm at the detector. Temporal resolution was tested

with an 80-ps laser pulse. Although the test was limited by the pulse power supply used to activate the MCP, resolution was much better than 1 ns.

Figure 6 shows a typical result obtained from the MCP diagnostics, in this case a time sequence of x-ray photographs of a neon plasma imploded with the ZAPP device. (The time direction is to the right.) The frames were exposed at intervals of 2 ns; the exposure time for each was 2 ns. The last frame is time-integrated. Simultaneous measurements of the x-ray and ultraviolet spectra with other MCP devices enable us to determine the temperature and density of the plasma as it heats and cools.

With the ZAPP device, we can also inject a mixture of gases in the gas puff. For complicated plasmas, the radiation from a selected minor constituent provides a "fingerprint" that indicates temperatures and densities. With this capability and the new MCP diagnostics, we are advancing our understanding of the interactions of ions, electrons, and photons in dense plasmas.

Joint U.S.-Japanese Neutron-Source Program

Realizing the promise of fusion power will require many advances in materials science. Foremost is the need to understand the response of materials to irradiation with 14-MeV neutrons (those produced in fusion reactions). The Rotating Target Neutron Source II (RTNS-II), a materials test facility at LLNL dedicated to fusion materials research, has operated since early 1979 in support of the U.S. fusion power program. Although the facility contains two separate neutron sources, funding constraints made it possible to operate only one source.

These constraints were offset early in 1982, when the governments of the U.S. and Japan reached an agreement under which Japan contributes about $2 million per year to RTNS-II operations and shares the neutrons available for experiments. This arrangement will effectively double the RTNS-II budget, enabling us to start up the second neutron source. The resulting increase in operating hours and improved performance will triple the annual neutron output.

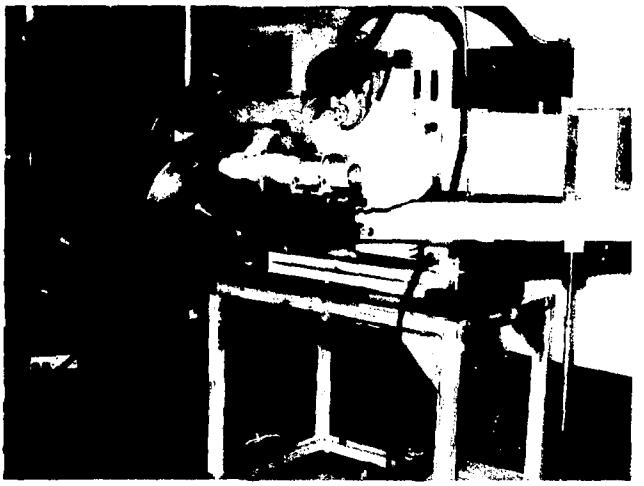

Fig. 7

Dr. Toshiyuki Iida of Osaka University, Japan, preparing fiber-optics material for the measurement *in situ* of light transmission in the RTNS-II target room. Dr. Iida is the first Japanese scientist assigned to work at RTNS-II. The 50-cm-diameter target is mounted on the red cone forming the end of the deuteron beam line.

At the RTNS-II, we produce neutrons by accelerating deuterium ions to 400 keV and transporting the beam to a rotating target coated with metal tritide (Fig. 7). The deuterons in the beam fuse with the tritium in the target to create 14-MeV neutrons. To dissipate the enormous power density deposited by the deuteron beam, we rotate the target at 5000 rpm. Early operations were done with targets 23 cm in diameter; in November 1981, we increased target diameters to 50 cm to allow the use of higher beam currents and to improve the target lifetime.

Japan's fusion technology program is developing rapidly. The joint U.S.-Japanese effort will enable the two countries to merge their programs in the area of fusion neutron effects and will give Japan immediate access to an advanced experimental facility. Japanese scientists are now in residence at RTNS-II, conducting experiments and working with U.S. colleagues. Japan is also developing a substantial postirradiation test laboratory at the facility. The

laboratory, which will eliminate most shipping time and unnecessary handling of radioactive materials, will be used jointly.

A bilateral RTNS-II Steering Committee charts the course of the experimental program and the general development of RTNS-II. Early in 1982, the committee held its first meeting at Monbusho, the Tokyo headquarters of the Japanese agency that supports the RTNS-II research, to plan for the coming year.

New Satellite Data Links for Fusion Research

The National Magnetic Fusion Energy Computer Center (NMFECC), with headquarters at LLNL, recently completed conversion of its communication system to a satellite service. The new service replaces a 50-kbit/s dedicated Bell System land line that had been in use since 1976. Satellite communications now link service centers throughout the country at a significant reduction in operating costs (Fig. 8).

NMFECC supports the nationwide magnetic fusion energy research program by providing the large-scale resources of a CDC-7600 and two Cray 1 computers.[1] Some 1600 MFE researchers across the country enjoy access to the computer center via a data communications network designed, installed, and operated by the NMFECC staff. The network consists of data links from NMFECC headquarters at LLNL to remote user sites, including Hanford Engineering Development Laboratory, Science Applications, Inc., General Atomic Corporation, the Lawrence Berkeley, Los Alamos, and Oak Ridge National Laboratories, Princeton Plasma Physics Laboratory, the Universities of California (Berkeley and Los Angeles), Washington, Texas, Illinois, and Wisconsin, and Stanford, New York, and Cornell Universities.

A 56-kbit/s satellite link between NMFECC and the Princeton Plasma Physics Laboratory was established in April 1981. The remaining three links (to Oak Ridge, Los Alamos, and General Atomic) were completed on an accelerated schedule by January 1982. By freeing NMFECC from dependence on a land-line system, for which higher tariffs were recently announced, the new satellite service will reduce operational costs to only about a half or a third of the increased cost of the older service. The annual savings to the national MFE program will be nearly $500 000.

The change to satellite communications was based on studies that showed such links would be more available, more reliable, less expensive, and faster (up to 256 kbit/s) than land lines. The new system required some accommodating software changes. As the satellite circles in a geosynchronous orbit at an altitude of about 35 400 km, there is a delay of about 0.5 s from the time data are sent over the link until an acknowledgement is received from the other end. The sender must hold data during this time. In addition, because effective utilization requires that the link must be kept busy, the sender must keep 0.5 s worth of data "in the air" at any given time. Although the propagation delay must be accounted for in the communication protocols, this has not posed a significant technical problem.

Before the linkup to the satellite system, NMFECC developed and installed two delay simulators in a local communications link to test their effect on the software. The testing revealed some problems, which were corrected before linkup. The link to the Princeton Laboratory went into operation on the first day the service was made available and has remained on line ever since. NMFECC's experience with the satellite communications system to date has provided one of those rare occasions on which performance exceeded our expectations at reduced costs.

Terrestrial lines for data communications links shorter than a few hundred miles or at bandwidths lower than 56 kbit/s are still competitive, but broadband communications via satellites currently offer overwhelming cost and technical advantages at longer distances and wider bandwidths.

Modeling EMP Damage to Semiconductors

Many components of both military and civil electronic devices are vulnerable to the sudden intense burst of electric and magnetic fields known as EMPs (electromagnetic pulses) that accompany nuclear explosions, lightning flashes, and the passage of a radar beam. Effective protection could be provided in many cases by enclosing the components in a metal shield, were it not for the fact that electrical leads usually must be run through the shield to connect the electronics inside with other components outside. These leads provide a ready path for the entry of EMP-induced currents. An EMP can also be created inside the shield if nuclear radiation passes through it, inducing currents in the internal wiring.

These considerations make it extremely difficult to shield electronic components effectively. Any scheme for hardening electronic systems against EMPs must therefore include the components themselves. We are conducting a study for the Air Force to find ways of hardening semiconductor p-n junction devices (i.e., those containing a permanent dipole charge layer), which are among the most vulnerable electronic components.

Our approach is to assess both the known mechanisms that can cause damage to p-n junction devices in an EMP environment and the existing models for these mechanisms. The objective is to extend or modify existing models so that they can accurately predict the input power threshold for device failure.

When a strong current pulse enters a semiconductor device, the immediate effect (first breakdown) is an avalanche of electrons and holes, producing an abnormally high current through the device. It is the ensuing second breakdown, however, that does the damage. There are two modes of second breakdown. The mode thought to predominate is thermal second breakdown, in which the current from avalanche first breakdown reaches a quasi-equilibrium that is maintained long enough to cause significant heating of the semiconductor. If the heating persists beyond the point where thermal current runaway occurs, the resulting rapidly increasing currents and temperatures can damage or destroy the semiconductor by creating hot spots in the junction

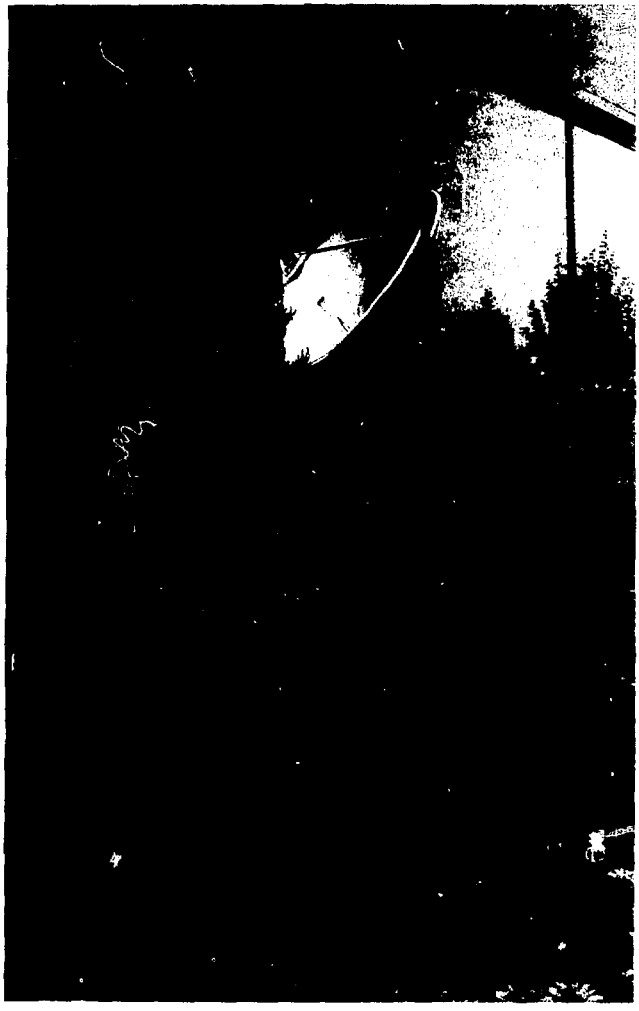

Fig. 8

Parabolic antenna (one of two) recently installed at the LLNL headquarters of the National Magnetic Fusion Energy Computer Center. This satellite communications system (56-kbit/s) links remote user sites throughout the country at a significant reduction in operating costs.

Fig. 9

Computer plots of the development of a hot spot and current filament during thermal second breakdown in the junction region of a diode. At 10 ns after the current pulse arrives, avalanche breakdown begins to raise the current density passing through the semiconductor. (a) By 400 ns, the junction region is being heated uniformly over its entire surface by a uniform current density. (b) Before a critical temperature between 600 and 800 K is reached, heating is still uniform. (c) After the critical temperature is exceeded, temperature and current density start to increase disproportionately in the central region, forming the beginning of a hot spot. (d) The temperature and current density profiles have both collapsed into the center of the device, creating a hot spot and a current filament. Should the temperature rise much further, it will exceed the melting point (1683 K), and the semiconductor will be damaged or destroyed.

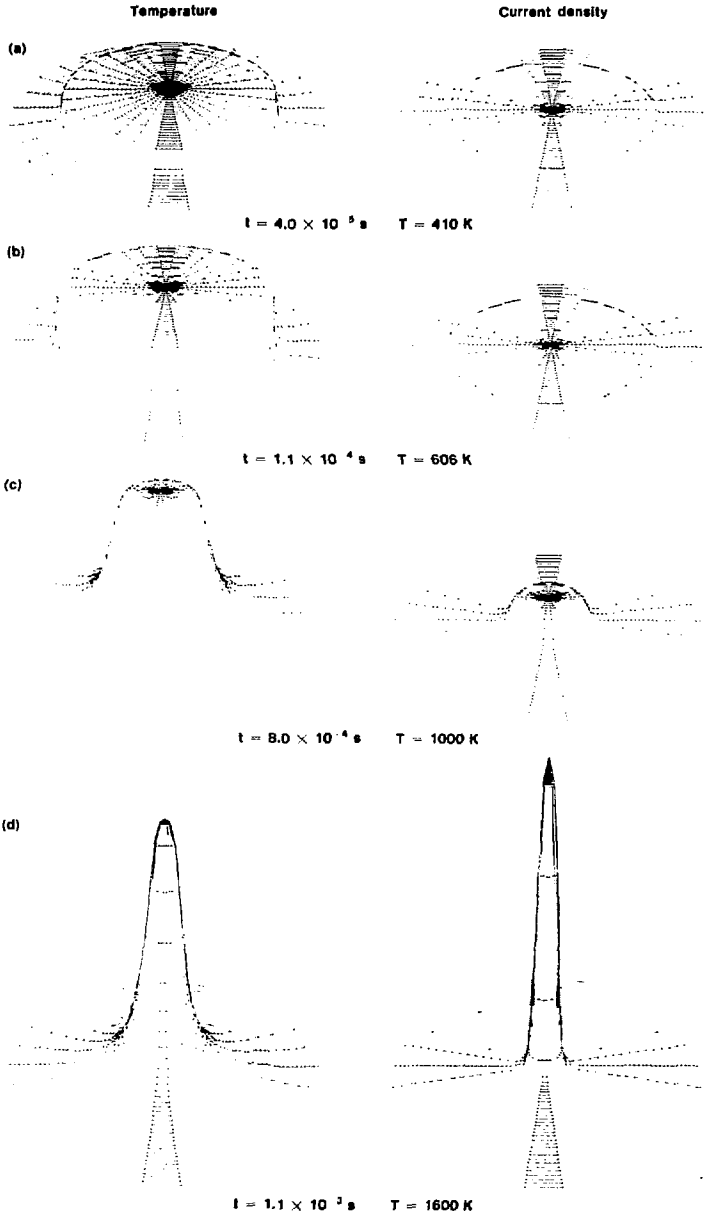

region. Figure 9 shows a sequence of computer simulations of a developing hot spot and current filament during thermal second breakdown.

The other type of second breakdown is current-mode second breakdown. It can occur in transistors when the current from avalanche breakdown does not level off at a temporary equilibrium but continues to increase—due to injection of holes and electrons from the emitter and collector of the transistor—until it may produce damaging hot spots in the junction region.

Which mode of second breakdown occurs is a function ot the energy of the EMP-induced pulse. Below a certain energy, the avalanche breakdown current will level off at a quasi-equilibrium and the second breakdown (if it occurs) will be thermal breakdown. Above that energy, the avalanche breakdown current will not reach equilibrium but will continue to increase, bringing on current-mode second breakdown. The two modes of second breakdown can be distinguished by their different rates of development. Current-mode second breakdown develops much faster—in nanoseconds, compared with microseconds for thermal second breakdown.

Our assessment of existing models for second-breakdown phenomena led us to conclude that none of them is accurate enough to predict failure thresholds for p-n junction devices. Therefore, we developed two computer models of our own. The first is a cylindrical, two-dimensional, time-dependent model that represents a p-n junction operating in a strong electromagnetic field. It is useful for analyzing p-n junction diodes. The other is a one-dimensional, time-dependent model of a transistor. Both models numerically solve the time-dependent equation for thermal energy transport and the nonlinear, time-dependent transport equations for electrons and holes.

The results of the calculations are displayed as plots of current and voltage as a function of time and as plots of current density and temperature as a function of position. From the current and voltage plots, we can determine the input power and power duration required to produce failure of the device in different internal and external environments. We will be able to compare these results with experimental results for commercial devices, which should enable us to refine the models and develop confidence in them.

As it stands, our model of a p-n junction device is a relatively fast method of examining the sensitivity of thermal-second-breakdown power levels and times to the various device parameters. This model is giving us more insight into the behavior of these devices in the second-breakdown regime. Likewise, the transistor model is giving us insight into the conditions under which current is generated and injected to produce current-mode second breakdown.

We plan to extend our computer models to three dimensions in a cylindrical geometry and to two or three dimensions in a rectangular geometry. These changes will enable us to consider more complex device shapes and to examine more accurately the effects of current-mode second breakdown. Our goal is to define the parameters that enhance the survivability of a semiconductor device during an EMP-induced transient.

Key Words: electromagnetic pulse (EMP); exploding bridgewire; diamond turning—optics; hardening—electronics, semiconductor, transistor; image-converter camera; laser optics; lathe—diamond; National Magnetic Fusion Energy Computer Center (NMFECC); multichannel plate; Nova; Novette; optical fiber; optrode; potassium dihydrogen phosphate (KDP); precision measurement; Raman fluorescence; Rotating Target Neutron Source II (RTNS-II); satellite data link; Z-pinch Atomic Physics Project (ZAPP).

Notes and References

1. *Energy and Technology Review*, December 1981 (UCRL-52000-81-12), p. ii.
2. For additional details about ZAPP, see the July 1981 *Energy and Technology Review* (UCRL-52000-81-7), p. 12.
3. See *Energy and Technology Review*, July 1981 (UCRL-52000-81-7), p. 42, for more information on the NMFECC.

Past Titles

Articles published in recent issues of the *Energy and Technology Review* are grouped below mainly according to their chief sponsors, the Assistant Secretaries of the U.S. Department of Energy. Research funded by other Federal agencies is listed under Work for Others.

ENERGY RESEARCH

Successful MFTF-B Technology Demonstration (Brief—May 1982)
Composite-Material Flywheels and Containment Systems (March 1982)

DEFENSE PROGRAMS

Inertial Fusion

Measuring Microsphere Targets for Fusion Experiments (June 1982)
Damage-Resistant Antireflection Surfaces for High-Power Lasers (March 1982)
Measuring the Microtopography of Optical Surfaces (March 1982)
The Free-Electron Laser Amplifier (January 1981)

Military Application

New Cable Emplacement Device Tested (Brief—June 1982)
The Raman Spectroscopy Microprobe (June 1982)
Slow Positrons from the 100-MeV Linac (Brief—April 1982)
The Geology of Yucca Flat (April 1982)
The LLNL X-Ray Calibration and Standards Laboratory (February 1982)
Ion-Atom Interactions (January 1982)

LABORATORY HISTORY

Thirty Years Ago: Controlled Thermonuclear Reactions (June 1982)
Moving In . . . (February 1982)

LABORATORY REVIEWS

U.S. Oil Supply Reflects World Events (Brief—May 1982)
How Vulnerable Are U.S. Sources of Strategic Materials? (February 1982)

WORK FOR OTHERS

Department of Defense

Improving Tank Track Pads (May 1982)
Generating Intense Electron Beams (December 1981)

Environmental Protection Agency

Atmospheric Ozone: Zeroing In (May 1982)

National Institutes of Health

Slit-Scan Flow Cytometry: A Promising New Cytometric Tool (April 1982)
The Solid-State Automated Microscope (January 1982)

Nuclear Regulatory Commission

Nuclear Waste Storage: Evaluating the Uncertainties (May 1982)
Earthquake Safety of Nuclear Power Plants (April 1982)

Disclaimer

Printed in the United States of America
Available from
National Technical Information Service
U.S Department of Commerce
5285 Port Royal Road
Springfield, Virginia 22161
Price: Printed Copy $7.00, Microfiche $3.50

Art Credits

Page 1. Scott Dougherty
Page 7. George P. Dooley
Page 14. Scott Dougherty
Page 23. John P. Pena
Page 41. Brett Clark

U.S. Government Printing Office: 1982/7 - 587-055/32

Technical Information Department · Lawrence Livermore National Laboratory · University of California · Livermore, California 94550